



Original Paper

Update and Review of Continental Conductive Surface Heat Flow Measurements in México: An Analysis of Deep Boreholes

O. M. Espinoza-Ojeda^{1,4,5}, R. M. Prol-Ledesma^{2,4} and J. A. Muñiz-Jauregui³

Received 11 August 2022; accepted 28 February 2023
Published online: 24 March 2023

Conductive heat flow is an important parameter that is used to explain, directly or indirectly, several geological, geophysical and geochemical processes in the Earth's interior. It is also one of the main input parameters for reliable estimations of resources related with geothermal and petroleum systems. That is because heat flow is used to describe subsurface temperature profiles and heat transfer mechanisms, thereby enabling the establishment of heat storage reserves in the case of geothermal systems and conditions of thermal maturation of organic matter in petroleum genesis. Since 2014, collection of data to estimate new continental conductive heat flow values in México has been an exhaustive scientific task. As a result, data from 4159 sites have been compiled, mostly from deep geothermal and petroleum boreholes. In this context, only 3,888 new geothermal gradient data were compiled and used to estimate new heat flow values. These new values complement the 702 continental heat flow values compiled and published between 1974 and 2021. Traditionally, all efforts to measure geothermal gradient in México have focused on the five high enthalpy geothermal fields under exploitation. Therefore, this continuous updating of the continental heat flow database would be an excellent input for Geothermal Play Fairway Analysis, enabling to define areas at a regional level with thermal anomalies and discovering new prospects, resulting in better knowledge of Mexican geothermal resources. Finally, the obtained data will help interested private and public entities to improve the geothermal exploration techniques in collaboration with academic institutions. Moreover, the scientific community interested in Earth science studies will benefit from this information with application to diverse research that involves the thermal evolution of the crust.

KEY WORDS: Heat flow, Geothermal energy, Geothermal boreholes, Petroleum boreholes, Thermal profiles, Geothermal plays, México.

¹CONACYT, Instituto de Investigaciones en Ciencias de La Tierra, Universidad Michoacana de San Nicolás de Hidalgo, 58060 Morelia, Michoacán, Mexico.

²Instituto de Geofísica, Universidad Nacional Autónoma de México, CDMX 04510 Mexico, Cd. Universitaria, Mexico.

³Escuela Nacional de Educación Superior Unidad Juriquilla, Universidad Nacional Autónoma de México, Boulevard Juriquilla 3001, 76230 Santiago de Querétaro, Querétaro, Mexico.

⁴Centro Mexicano de Innovación en Energía Geotérmica (CemieGeo), Carretera Tijuana-Ensenada No. 3919, Zona Playitas, 22860 Ensenada, Baja California, Mexico.

⁵To whom correspondence should be addressed; e-mail: ome-spinozaoj@conacyt.mx

INTRODUCTION

For suitable estimation of energy resources in geothermal systems, a most realistic conceptual model must be developed, which depends on an assertive study and understanding of several geological, geophysical and geochemical parameters involved in such systems (e.g., Avellán et al., 2018; Jácome-Paz et al., 2019; Almaguer et al., 2020; Sena-

Lozoya et al., 2020). A particularly important geophysical parameter is heat flow, which is required to estimate the heat stored in the subsurface, which in turn can be exploited to produce electrical power and/or for direct geothermal uses (Fuchs et al., 2020; Guerrero-Martínez et al., 2020).

Tectonic evolution makes México a privileged country regarding geothermal energy, i.e., large-scale geodynamic phenomena linked to subduction, extensional lithosphere activity, volcanism and major fault systems, among others, considered as some of the main originators of crustal thermal anomalies (e.g., Ferrari et al., 2007, 2012; Campos-Enríquez et al., 2019; Busby et al., 2020). Nowadays, only five developed Mexican high enthalpy geothermal fields (Cerro Prieto, Los Azufres, Los Humeros, Tres Vírgenes and Domo San Pedro) have an installed capacity of 962.7 MWe (Think GeoEnergy, 2023). However, the country can increase its potential to produce geothermal energy due to more than 4,000 thermal manifestations of low- and medium-enthalpy systems across the country (Iglesias et al., 2015), e.g., Los Cabos, Guaymas; Cuitzeo, Rancho Nuevo, (Hernández-Morales and Wurl, 2017; Almirudis et al., 2018; Gutiérrez-Negrín et al., 2020; Landa-Arreguín et al., 2021). Moreover, the Mexican geothermal potential probably can be accentuated by the existence of blind or hidden geothermal systems (Prol-Ledesma, 2000; Bâncora and Prol-Ledesma, 2008; Faults and Hinz, 2015; Dobson, 2016).

There is no trustworthy estimate of the actual geothermal potential of México, although some works have been published with related information through the study of heat flow, geothermal gradient or subsurface temperature maps (Blackwell and Richards, 2004; Iglesias et al., 2016; Prol-Ledesma & Morán-Zenteno, 2019). However, these records must be constantly updated. The heat flow pioneering works date back to more than 40 years ago (e.g., Smith, 1974; Smith et al., 1979; Reiter & Tovar, 1982; Ziagos et al., 1985). More recently, some Mexican research projects, focused on analyzing and estimating the geothermal reserves in México, have published heat flow measurements obtained from geothermal and petroleum exploration boreholes (e.g., Prol-Ledesma et al., 2016; Espinoza-Ojeda et al., 2017a, b; Prol-Ledesma et al., 2018).

Hence, this work's main objective was to present an updated heat flow database for México, as well as updated geothermal gradient and heat flow maps. To accomplish this objective, 4,159 drilling

reports of deep geothermal and petroleum boreholes were processed to compile thermal logs (transient borehole temperature (TBT) and bottom-hole temperature (BHT)) and rock formation stratigraphy. A rigorous quality assessment of the data produced 3,888 new heat flow values that were added to the 702 continental heat flow values compiled and published previously between 1974 and 2021 (Smith, 1974; Smith et al., 1979; Reiter & Tovar, 1982; Ziagos et al., 1985; Blackwell & Richards, 2004; Prol-Ledesma et al., 2016; Espinoza-Ojeda et al., 2017a, b; 2018; 2021).

METHODOLOGY

Technical reports from 4,159 sites were compiled, including geological and thermal geophysical data. All the information was provided by the Comisión Federal de Electricidad (CFE-Mexican Government Electricity Company) and Petróleos Mexicanos (PEMEX-Mexican Government Oil Company). The methodology proposed by Espinoza-Ojeda et al. (2017b) and Prol-Ledesma et al. (2018) which consists of data collection and processing to estimate new heat flow values was applied to the gathered data; the main tasks were as follows:

- (1) Update the stratigraphy database and the TBT and BHT data from drilled deep boreholes. The stratigraphic profile database was obtained from the drilling stage reports provided by CFE and PEMEX. TBT data include logs of temperature, depth and thermal recovery time. BHT was recorded at the deepest part of a borehole when the drilling process was stopped at different depths. BHT data were corrected using eight correction methods (Table 1): AAPG; FM; FMD; FMC; HC; KC; FM-SMU; and COG.
- (2) Update the continental heat flow database of México. The calculation of the new conductive surface heat flow values was carried out using the Bullard (1939) method. A statistical analysis to discard boreholes with convection disturbances was applied.
- (3) Elaborate new geothermal gradient and heat flow maps of México. The results of two interpolation methods and analysis of the interpolation error are presented here.
- (4) Geothermal Play Fairway Analysis. Application of this regional exploration method was

Table 1. Summary of BHT correction methods used in this work

Method	Equation of correction	Source
Average AAPG (AAPG)	$\Delta T = (1.878 \times 10^{-3})z + (8.476 \times 10^{-7})z^2 - (5.091 \times 10^{-11})z^3 - (1.681 \times 10^{-14})z^4$	AAPG (1976)
Förster/Merriam (FM)	$\Delta T = (0.012)z - 3.68$	Förster & Merriam (1995)
Förster/Merriam/Davis (FMD)	$\Delta T = (0.0127)z - 7.64$	Förster et al. (1995)
Förster/Merriam Censored (FMC)	$\Delta T = (0.021)z - 13.54$	Förster et al. (1995)
Harrison correction (HC)	$\Delta T = (0.0183)z - (2.34 \times 10^{-6})z^2 - 16.512$	Crowell et al. (2012)
Kehle correction (KC)	$\Delta T = (4.375 \times 10^{-3})(0.3048z) - (2.143 \times 10^{-8})(0.3048z)^2 - (8.819 \times 10^{-12})(0.3048z)^3 - 1.018$	Crowell et al. (2012)
FM modified by SMU Geothermal Laboratory (FM-SMU)	$\Delta T = (0.017)z - 6.58$	Crowell et al. (2012)
Crowell/Ochsner/Gosnold (COG)	$\Delta T = (0.0124)z + 7.8825$	Crowell et al. (2012)

z is the BHT depth in meters

attempted using the new heat flow data to define undiscovered prospective areas.

Database

Figure 1 presents the locations of sites that comprise the new heat flow database created from the TBT and BHT records from 3,888 drilled deep boreholes. Also, 1107 published offshore sites (inside the exclusive economic zone) are included in Figure 1 to visualize their distribution and covered areas (e.g., Von Herzen 1963, 1964; Epp et al., 1970; Erickson et al., 1972; Henyey & Bischoff, 1973; Lawver et al., 1973, 1975; Lee & Henyey, 1975; Lawver & Williams, 1979; Williams et al., 1979; Becker, 1981; Lonsdale & Becker, 1985; Prol-Ledesma et al., 1989; Khutorskoy et al., 1990; Becker & Fisher, 1991; Sanchez-Zamora et al., 1991, 2013, 2021; Nagihara et al., 1996; Fisher et al., 2001; Blackwell & Richards, 2004; Rosales Rodríguez, 2007; Espinoza-Ojeda et al., 2017a; Neumann et al., 2017; Negrete-Aranda et al., 2022; Peña-Domínguez et al., 2022). The new database includes TBT and BHT measurements from 14 geothermal and 3857 petroleum boreholes, 17 of which are offshore; see Figure 2 for an illustration of the T - z (temperature–depth) logs of geothermal and petroleum boreholes used in this study. The rock lithology profile database was updated with the technical drilling reports that supplied 188 stratigraphic profiles: 29 from geothermal and 159 from petroleum boreholes. Figure 3 displays a histogram of the reported total

depth of the compiled and analyzed boreholes in this study.

BHT data are measurements logged during thermal disturbance generated by drilling process; therefore, they must be corrected to determine the formation temperature. The BHT collected data do not have an associated drill stem test (DST) record because formation temperature is obtained commonly from DST data; hence, calculation of formation temperature was through the application of few correction methods.

The correction methods applied for BHT (Table 1) are a function of depth and do not depend on other parameters (e.g., drilling mud circulation time, thermal recovery time, borehole size, some thermophysical properties of the formation rock or drilling fluid, etc.). These methods have already been evaluated and applied in various studies, and reliable results were obtained even in areas other than those for which they were determined (e.g., Deming, 1989; Förster et al., 1995; Crowell et al., 2012). In our case, we did not have enough data to calibrate those methods and it is likely that some methods would underestimate or overestimate the formation temperature after BHT correction. For that reason, we defined an “apparent” formation temperature as the average of corrected BHTs with the methods in Table 1 (see Fig. 2), thus:

$$\text{BHT (corrected)} = \text{BHT} + \Delta T \quad (1)$$

where BHT (°C) is the actual temperature logged during drilling process and ΔT (°C) is the differential of temperature to correct the BHT and, thus, to estimate formation temperature.

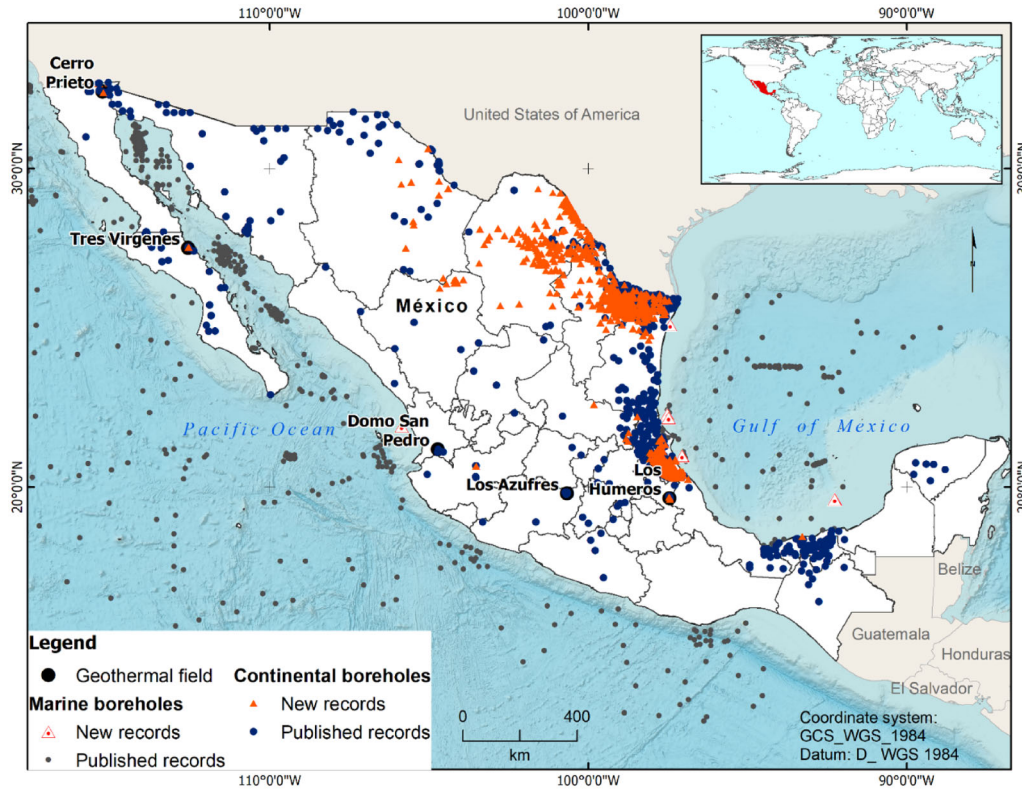


Figure 1. Updated continental heat flow database of México (orange filled triangles = new heat flow sites, blue filled circles = published heat flow sites) including 1,04 published offshore sites (gray filled circles) and 17 new sites (red-white triangles). Locations of the Mexican geothermal fields (Cerro Prieto, Las Tres Vírgenes, Domo San Pedro, Los Azufres and Los Humeros), currently under power exploitation.

CONDUCTIVE HEAT FLOW

Fourier’s law describes conductive heat transport phenomena in solid materials; therefore, the heat flow is calculated as:

$$q = -k(dT/dz) \tag{2}$$

where q is heat flow (W/m^2), k is thermal conductivity ($W/m\ K$) and dT/dz is temperature gradient (also known as geothermal gradient: $^{\circ}C/m$). In an ideal case, when a purely conductive heat transfer exists between different materials, thermal conductivity variations are present. These variations are considered in the thermal resistance concept. Hence, the heat flow for a layered medium is calculated as:

$$q = \frac{[T(z_i) - T_0]}{R_i} \tag{3}$$

where $T(z_i)$ is temperature ($^{\circ}C$) logged at a specific depth, and R_i is thermal resistance (m^2K/W) that is defined as:

$$R_i = \sum_i^n \frac{\Delta z_i}{k(z_i)} \tag{4}$$

where Δz_i is thickness (m) of each layer and $k(z_i)$ is the thermal conductivity ($W/m\ K$) of that layer. From Eq. 3, the Bullard (1939) method is derived to estimate heat flow for an ideal case, thus:

$$T(z_i) = T_0 + q_0 R_i \tag{5}$$

where theoretically, a plot between $T(z_i)$ measurements and the summed thermal resistance R_i (m^2K/W) must show linear tendency. Hence, an extrapolation of the straight line allows the slope (surface heat flow: q_0) and intercept (surface temperature: T_0) values to be determined. If some values do not follow the linear pattern, the linear relationship between $T(z_i)$ and R_i is not valid; therefore, those values are defined as outliers or rejected data, which could be thermally disturbed by local convective

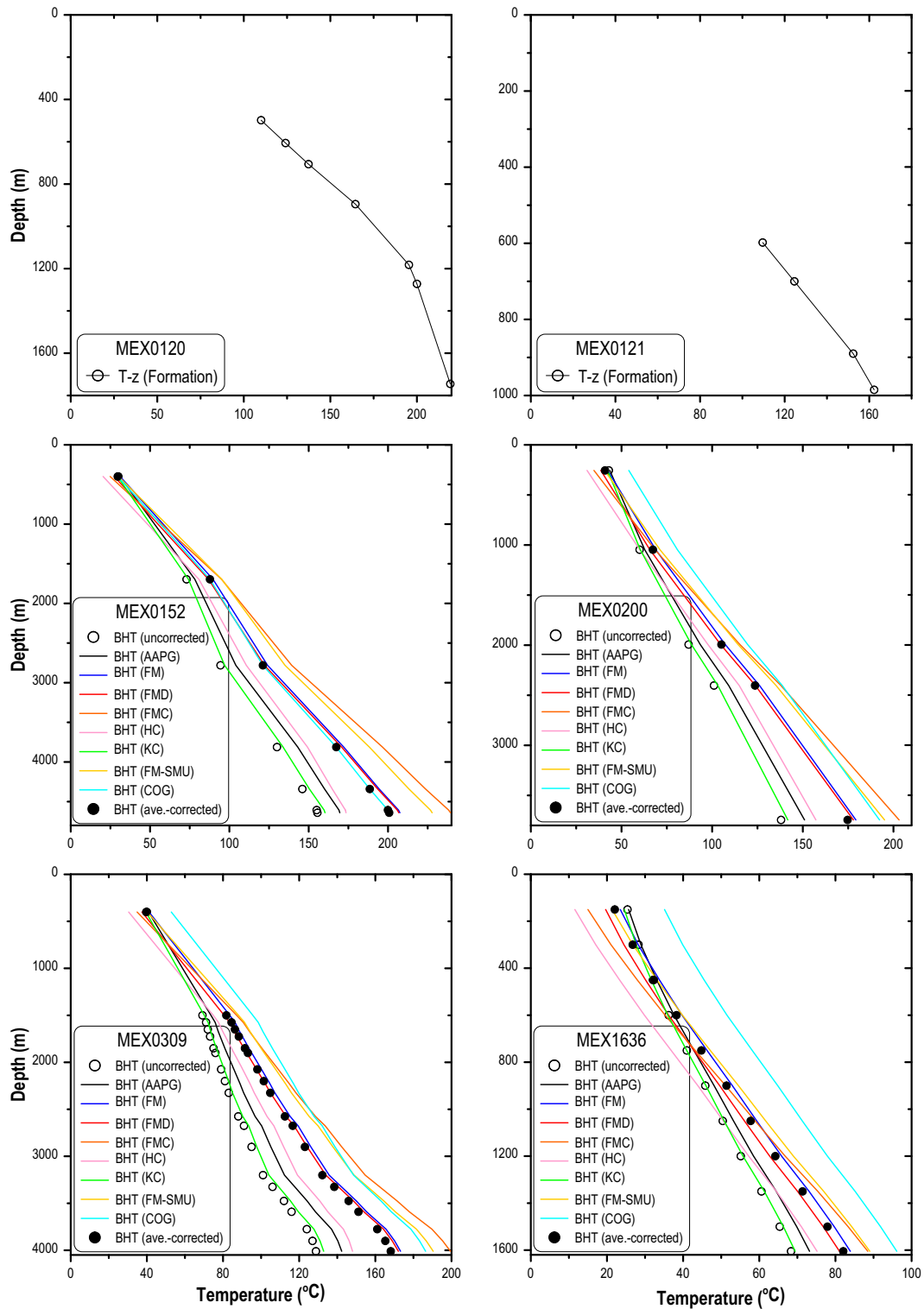


Figure 2. Plots of the temperature–depth profile ($T-z$) for six boreholes used for heat flow analysis. MEX0120-121 geothermal and MEX0152-0200-0309-1636 petroleum boreholes. BHT data corrected by different methods are included.

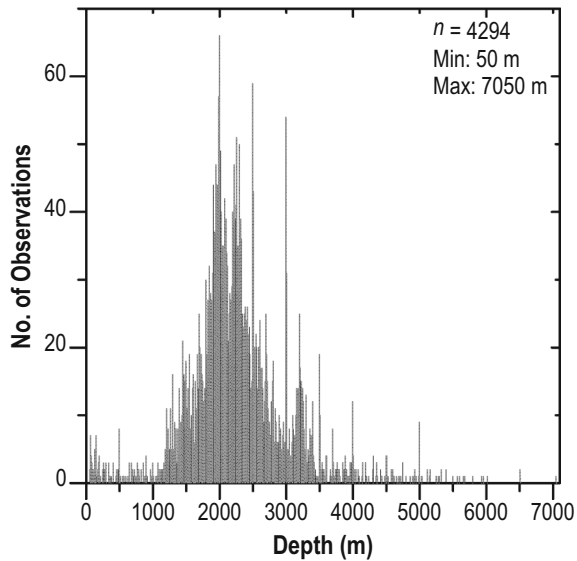


Figure 3. Histogram of reported total depth in the compiled and analyzed boreholes in this study. n is number of data.

effects, and most assuredly located within hydrothermal systems.

Commonly, a convective thermal disturbance can be thought of as a sudden or predominant warming (excessive rise) or cooling (temperature drop) of the temperature gradient, which would graphically observe as a “sharp” and major change in the slope of the gradient. In addition, heat flow affected by heat refraction was neglected in the country scale of this work due to the non-existence of considerable contrasts in thermal conductivities and/or geological structures heterogeneities (e.g., Jobmann & Clauser, 1994; Fulton & Saffer, 2009; Norden et al., 2012). In addition, as a test of linearity, the analysis of the coefficient of determination (R^2) to evaluate the variation between $T(z_i)$ and R_i to determine if linear regression model fits these parameters is suitable (i.e., $R^2 \approx 1$) (e.g., Miller & Miller, 2000; Bevington & Robinson, 2003). Therefore, if linearity deviation is present, the borehole is disturbed by a convection flow, and a low R^2 is calculated. Hence, undisturbed boreholes have correlation between T and z [i.e., $T-z$ plot] with an R^2 above 90% of confidence and, consequently, were considered for the construction of the heat flow database (e.g., Richards et al., 2012). Therefore, cases with R^2 below 90% of confidence are identified as disturbed thermal data and were discarded. All borehole data used in this study to calculate heat flow by the Bullard (1939) method satisfied the

parameter of reliability $R^2 \approx 1$ in the $T-z$ and $T(z_i)-R_i$ plots.

For illustration of the above principle, Figure 4 shows three geothermal boreholes. Figure 4a represents the $T-z$ and the Bullard plot for the borehole MEX0121, respectively. This case could be considered as purely conductive heat transfer because the linearity between $T-z$ and $T(z_i)-R_i$ is undisturbed; the R^2 value supports this statement. In the case of borehole MEX0128 (Fig. 4c, d), a semi-linearity in the $T-z$ and $T(z_i)-R_i$ plots is evident. The calculated R^2 and most data fall inside the 90% confidence limits, validating the predominant linearity in borehole MEX0128. Finally, borehole MEX0137 (Fig. 4e, f) is a representative example of a borehole perturbed by dominant convective heat transfer at depth. This case is representative of the 20 rejected boreholes that were excluded in the conductive surface heat flow database. However, surface temperatures of MEX0121 (Las Tres Virgenes, Figure 1), MEX0128 and MEX0137 (Los Humeros, Figure 1) were not reported. Based on surface temperature of 25 °C as reference datum that was assumed according to the National Institute of Statistic and Geography (INEGI, 2021), a high surface temperature is observed in Figure 4, except 4a, which fits the slope of the $T-z$ and $T(z_i)-R_i$ correlation. This indicates, despite having conductive thermal behavior of the thermal profiles, a thermal anomaly of a geothermal area.

Additionally, Figure 5 displays three different cases of petroleum boreholes. Figure 5a shows that temperature increases linearly with depth in borehole MEX0152 (central north of México); the $T-z$ linear relationship seems to be interrupted in the 2000–3000 m interval; even then, the linear tendency of the $T-z$ and $T(z_i)-R_i$ plots predominates in the R^2 analysis, where just one datum was rejected. In the second case, borehole MEX0200 (northeastern México: Fig. 5c, d) could be considered an ideal example of conductive heat transfer, according to the $T-z$ plot and the R^2 result of the Bullard plot. In the third case, borehole MEX0309 (central north of México: Fig. 5e, f) presents semi-linear temperature increases with depth. This semi-linear relationship is apparently preserved between the temperature and thermal resistance in the Bullard plot (Fig. 5f). In these cases, in relation to their location, a surface temperature of 25 °C was assumed (INEGI, 2021).

As final examples, Figure 6 represents ideal cases of conductive heat transfer, where linear relationship predominates in the $T-z$ and $T(z_i)-R_i$

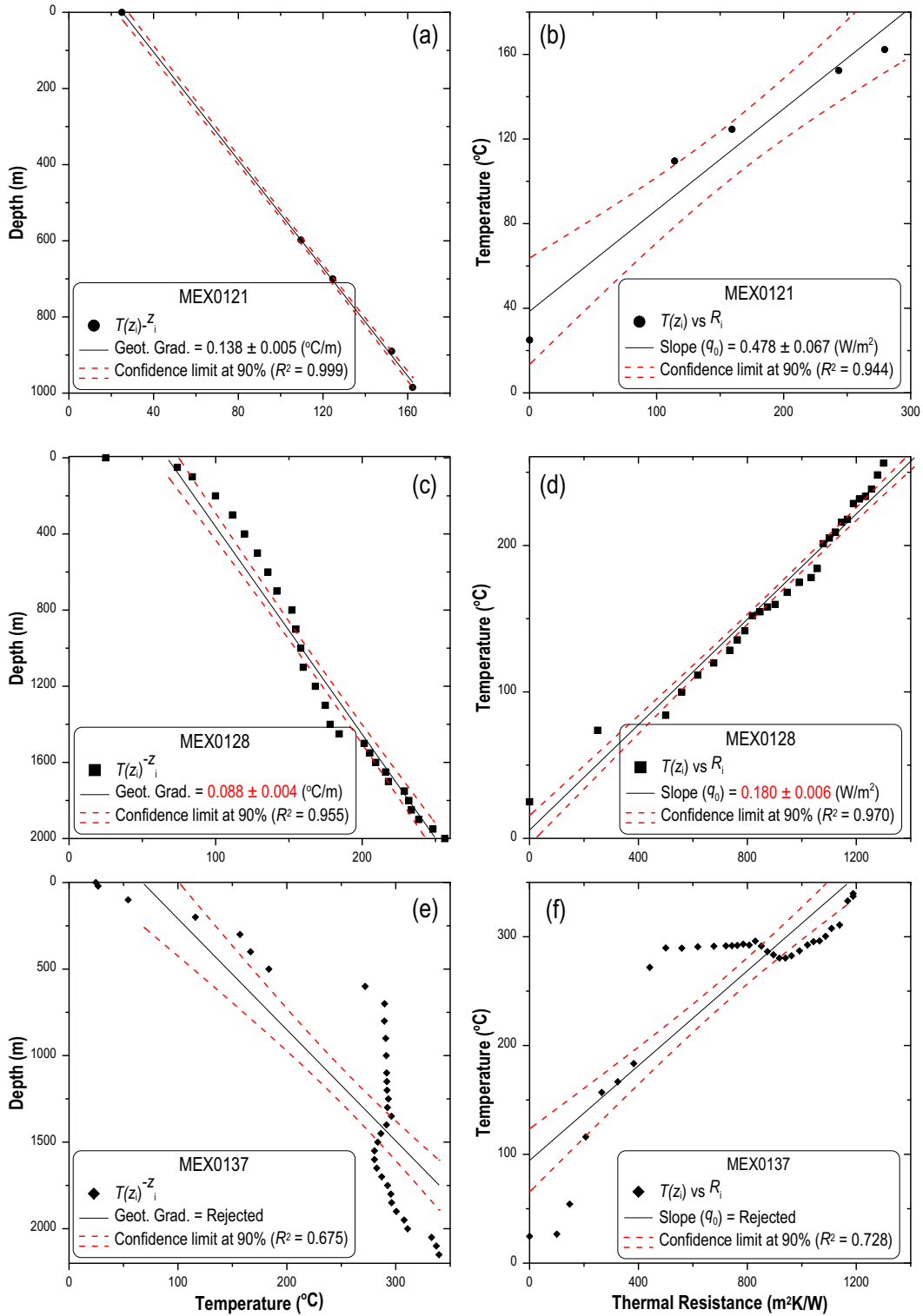


Figure 4. Borehole MEX0121: (a) temperature–depth profile; (b) Bullard plot. Borehole MEX0128: (c) temperature–depth profile; (d) Bullard plot. Borehole MEX0137: (e) temperature–depth profile and (f) Bullard plot.

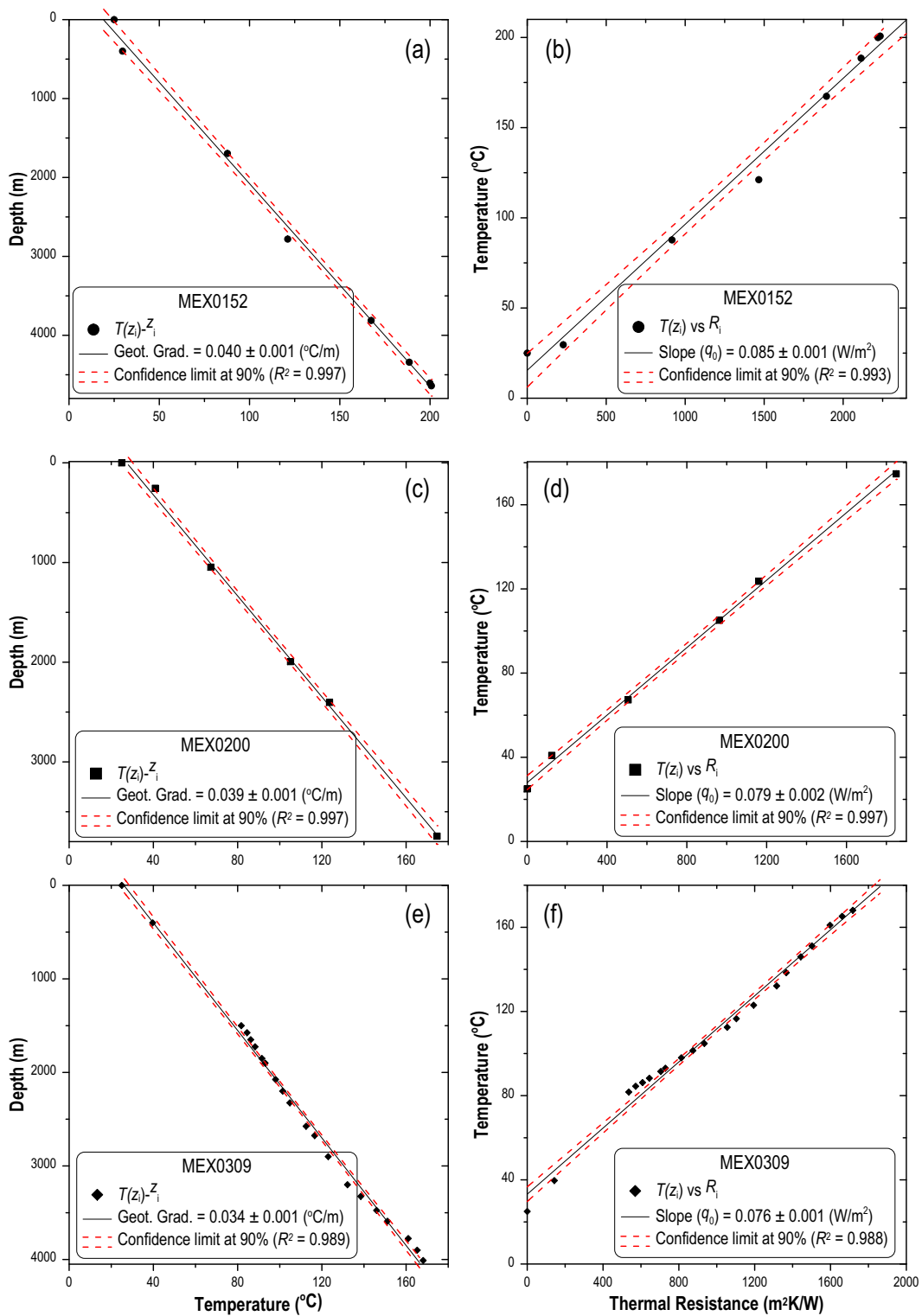


Figure 5. Borehole MEX0152: (a) temperature–depth profile, (b) Bullard plot. Borehole MEX0200: (c) temperature–depth profile, (d) Bullard plot. Borehole MEX0309: (e) temperature–depth profile and (f) Bullard plot.

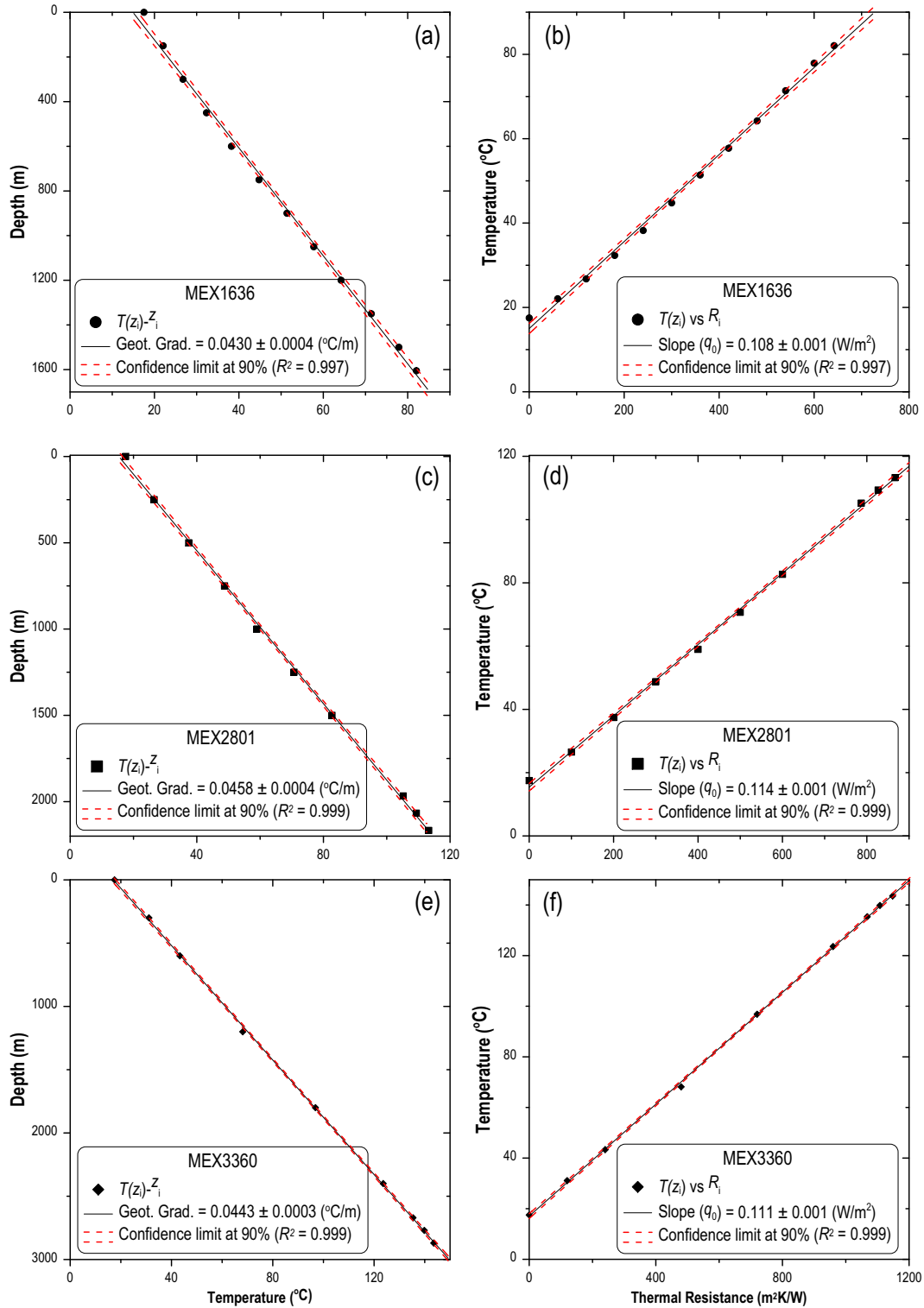


Figure 6. Borehole MEX1636: (a) temperature–depth profile and (b) Bullard plot. Borehole MEX2801: (c) temperature–depth profile and (d) Bullard plot. Borehole MEX3360: (e) temperature–depth profile and (f) Bullard plot.

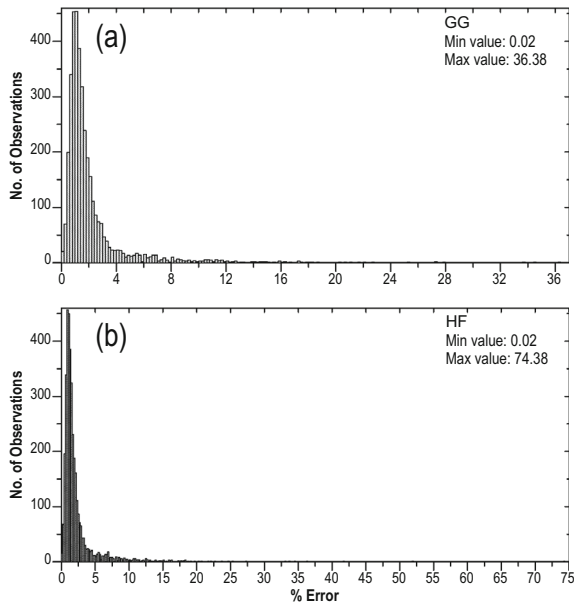


Figure 7. Histograms of percent error between estimated slope and its standard deviation: (a) geothermal gradient relative error (GG) and (b) heat flow relative error (HF).

plots, and the results are confirmed by the R^2 values. The petroleum boreholes MEX1636, MEX2801 and MEX3360 are located in central eastern coast of Mexico; hence, a surface temperature of 17.5 °C was assumed (INEGI, 2021).

In summary, Figure 4 represents the geothermal sites with predominant semi-linear and nonlinear relationships between $T-z$ and $T(z_i)-R_i$, indicating that most of them are perturbed by convection. As a result, 20 of the 37 analyzed geothermal sites were rejected. Petroleum borehole MEX0309 (Fig. 5e, f) is a representative example of petroleum cases with predominant semi-linear relationship between $T-z$ and $T(z_i)-R_i$. Finally, Figure 6 illustrates the $T-z$ and $T(z_i)-R_i$ plots from the MEX1636, MEX2801 and MEX3360 petroleum boreholes. Most of these examples represent the petroleum sites analyzed in this work, which describe an evident linear correlation between $T-z$ and $T(z_i)-R_i$.

Figure 7 displays the histograms of the percentage error for the geothermal gradient and heat flow estimations. It is shown that the relative errors are predominantly under 8% for the geothermal gradient estimations (Fig. 7a) and under 10% for the heat flow estimations (Fig. 7b). This empirical analysis supports the accuracy of the linearity anal-

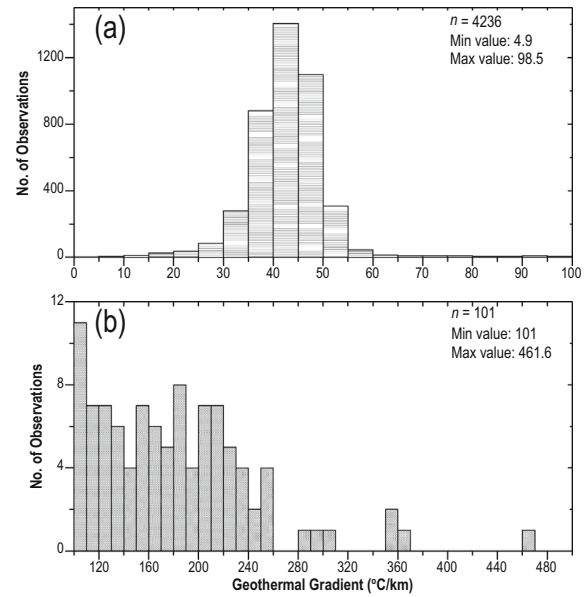


Figure 8. Histograms of updated continental geothermal gradient database of México. (a) Horizontal lines: values of 0–100 °C/km. (b) Diagonal lines: values of 100–500 °C/km. n is number of data.

ysis (R^2) because the results obtained show very low relative errors, meaning that in most studied sites conductive heat transfer predominates.

Interpolation

The development of the updated geothermal gradient and heat flow maps of México was achieved with interpolation data to describe different isotherms obtained from these two important parameters, according to their location and magnitude. Two interpolation methods were used to obtain the best results: inverse distance weighting (IDW) and empirical Bayesian kriging (EBK). The produced interpolation maps were constructed with SAGA software using 500×500 m cells.

IDW interpolation estimates the value of a point with a linearly weighted combination of a group of points (Bartier & Keller, 1996). IDW interpolation assumes that the variable being mapped decreases in influence at a greater distance from its sample location (Bartier & Keller, 1996; Setianto & Triandini, 2013). The IDW equation can be written as:

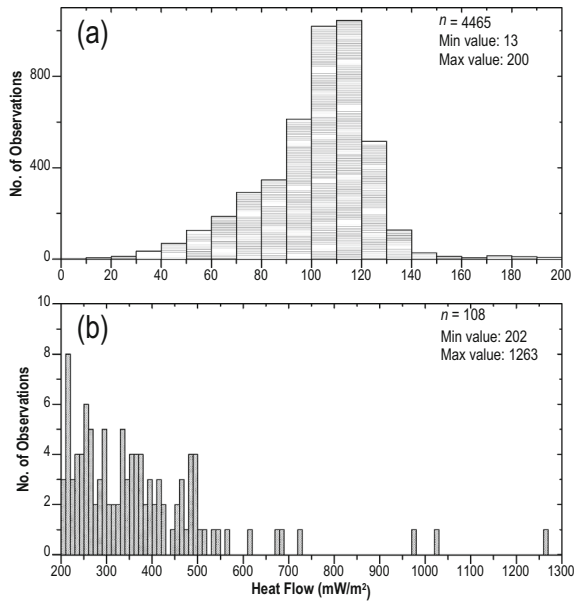


Figure 9. Histograms of updated continental heat flow database of México. **(a)** Horizontal lines: compiled heat flow values of 0–200 mW/m². **(b)** Diagonal lines: compiled heat flow values of 200–1300 mW/m². n is number of data.

$$q_{x,y} = \frac{\sum_{i=1}^n q_i d_{x,y,i}^{-w}}{\sum_{i=1}^n d_{x,y,i}^{-w}} \quad (6)$$

where $q_{x,y}$ is the point (unknown heat flow value) to be estimated at location x,y ; q_i represents the control value (known heat flow value) for the i th sample point; $d_{x,y,i}$ is the distance between $q_{x,y}$ and q_i ; w is the total number of predictions for each validation case defined by the user; and n is the number of control points nearest to the point being interpolated. By setting a high-power value, the closest points will have more influence for a better texture of the surface. As the power increases, the interpolated and the closest sample point values begin to approach each other. On the contrary, by specifying a lower power value, the surrounding points will take on more influence than those further away; this produces a smoother surface. Arguably, the optimal value for power is when the lowest minimum mean absolute error is considered (Bartier & Keller, 1996; Setianto & Triandini, 2013).

The EBK method provides an estimate at an unsampled site $q_{x,y}$ (unknown heat flow value), based on the weighted average of adjacent observed sites z_i (known heat flow value) within the study area (Pilz & Spöck, 2008; Setianto & Triandini, 2013).

The estimate of the weighted average given by the EBK predictor at $q_{x,y}$ is defined as:

$$q_{x,y} = \sum_{i=1}^n \lambda_i q_i \quad (7)$$

where λ_i is the weight assigned to each q_i and n represents the number of sample locations.

Finally, the R^2 was also used to evaluate interpolation error. This parameter determines the amount of variation between actual heat flow measurements and values estimated by interpolation, and it allows to determine the most suitable interpolation (i.e., when R^2 approaches 1).

Geothermal Play Fairway Analysis

In the petroleum industry, Play Fairway Analysis can be defined as a methodology that incorporates geological data at regional or local scale to improve knowledge for locating and prospecting a probable hydrocarbon reservoir, or as a combination of petroleum fields that are characterized by homologous geological conditions (e.g., Eguiluz-de Antuñano, 2009; Gutiérrez-Negrín, 2015; Shervais et al., 2017). Thus, a Geothermal Play Fairway Analysis (GPFA) can be defined as an exploration approach that integrates regional data to demarcate geothermal plays and it is an important tool for locating blind geothermal systems. The combination of geoscientific parameters for defining the heat source of geothermal energy systems may include heat flow, faults and fractures network related with permeability, and tectonic evolution (Moeck, 2014; Moeck et al., 2015). GPFA incorporates parameters as layers in a geographic information system (GIS). This approach reduces the risk of failure by defining local areas, which have high probability of hosting exploitable geothermal systems (Moeck, 2014; Moeck et al., 2015; Shervais et al., 2017, 2020).

In this study, we proposed the analysis of an area with a high density of heat flow values located in a region controlled by the same set of geological conditions. We compiled geodynamic elements that indicate the presence of geothermal potential (Shervais et al., 2020): subsurface thermal anomaly or thermal regime (possible heat source), fracture-related reservoir permeability, and accessible fluids. Heat flow data, fault systems, geological and tectonic events (recent volcanism) on a regional scale were compiled in a GIS with a data layer per indi-

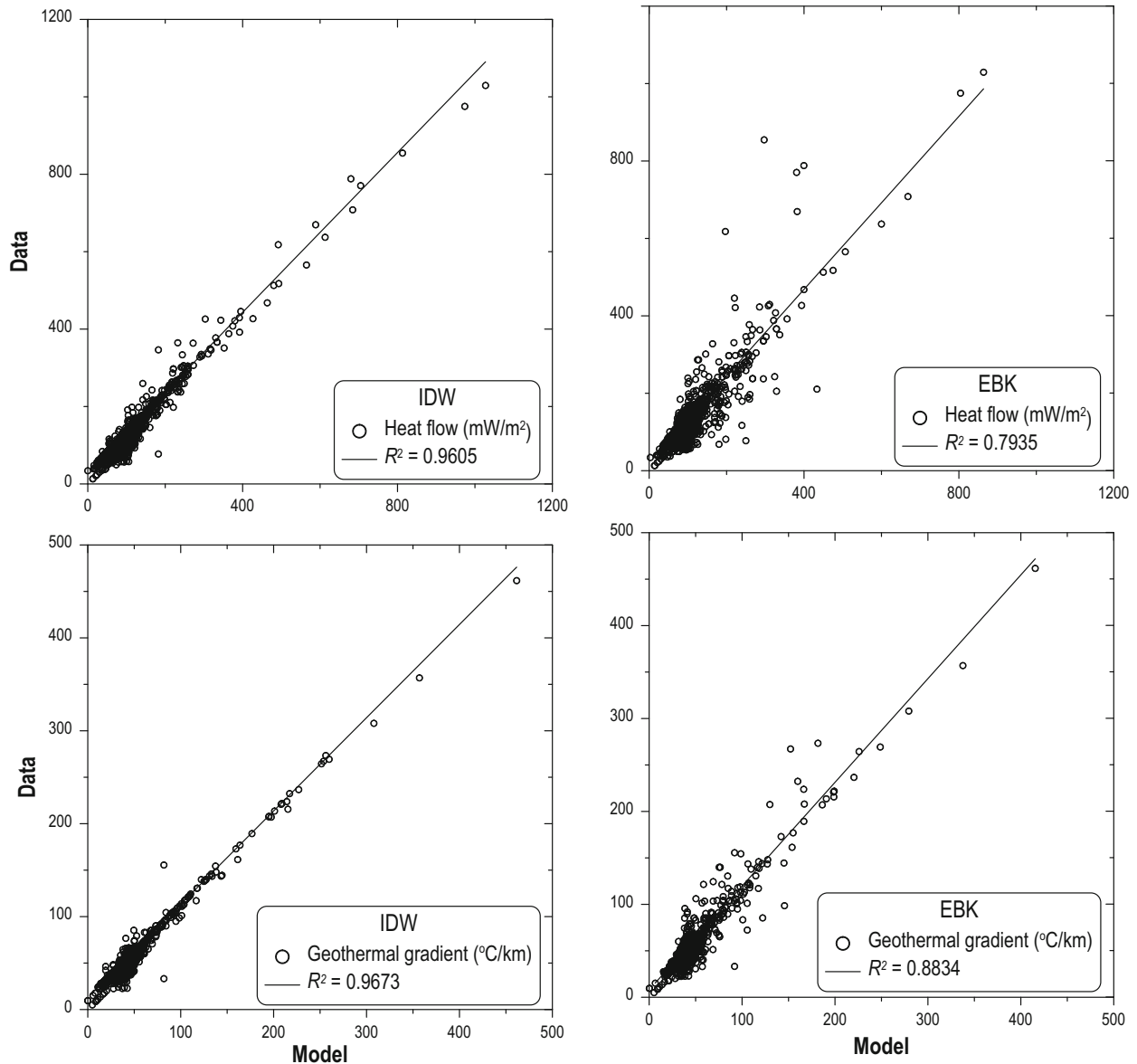


Figure 10. Accuracy comparison between IDW and EBK interpolation methods through correlation plots between actual data (heat flow and geothermal gradient) and modeled data by each method. Obtained R^2 is indicated for each analyzed case.

cator. In this work, recent volcanism (age ≤ 3 Ma) was considered because geothermal systems are frequently linked to regions of both active tectonism and volcanism, young plutonism (≤ 3 Ma) and crustal thinning (Moeck, 2014; Moeck et al., 2015).

RESULTS AND DISCUSSIONS

The Mexican heat flow database was updated with the newly estimated 3871 heat flow values from

702 previously published continental heat flow data; their locations are shown in Figure 1. As a result, the new database is an integration of 4573 continental heat flow measurements and 4337 geothermal gradient values (see Fig. 1). As important remark, the updated Mexican heat flow database contains 702 published (plus 1,084 offshore sites) and 3,888 new data (including 17 offshore sites). This database is compiled in a worksheet file, which contains two classification sheets, the “previous data” and the “new data.” An electronic worksheet file named

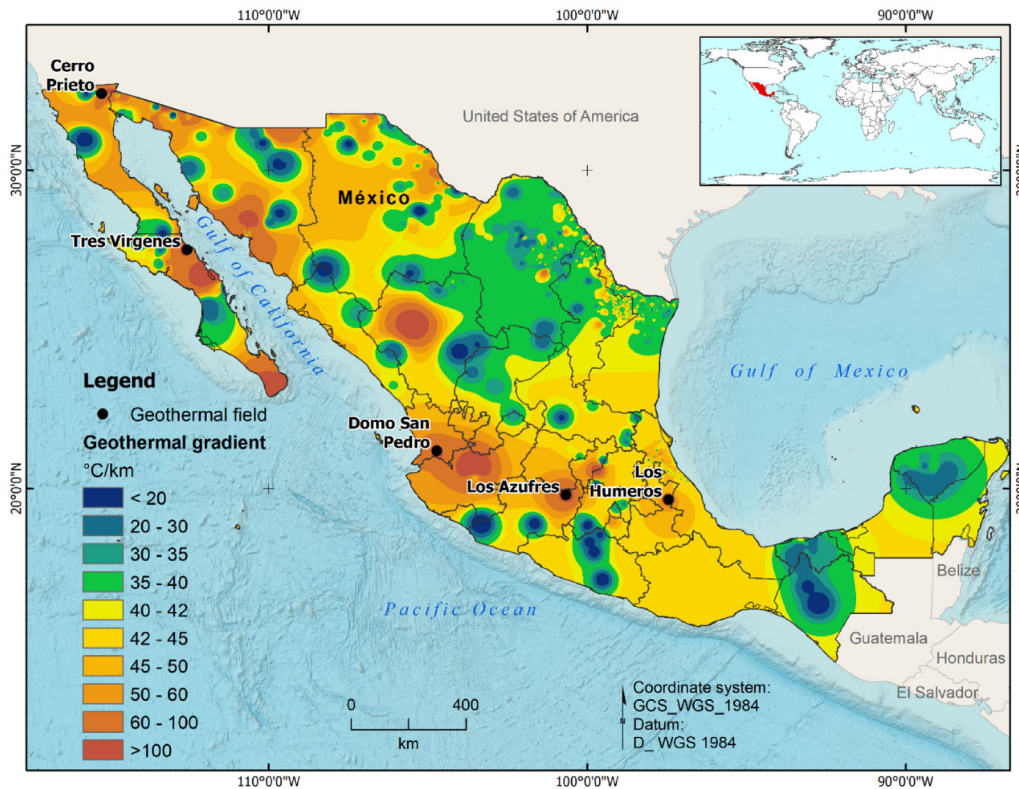


Figure 11. Continental geothermal gradient map of México (updated: 2022). Locations of the Mexican geothermal fields (Cerro Prieto, Las Tres Virgenes, Domo San Pedro, Los Azufres and Los Humeros) are shown as references of areas with known thermal anomalies.

“Mexico_HF_database (Espinoza-Ojeda et al., 2023)” can be downloaded from: https://github.com/omespinozajeda/Mexico_HF_database.git.

Figures 8 and 9 show the histograms for the available geothermal gradient estimations and the published and new heat flow values, respectively. Due to the large amount of data used for this work, the data were grouped in two energy level subsets to enable visualization of the data variation. In Figures 8 and 9, the non-uniform distribution of the updated database for geothermal gradient and heat flow values is evident. In Figure 8a, the most numerous geothermal gradient estimations are located in a 25–55 °C/km interval, which is broadly related to the 40–140 mW/m² heat flow interval (Fig. 9a) due to the direct proportionality between geothermal gradient and conductive heat flow. The histograms illustrated in Figures 8a and 9a, once again, demonstrate that México has a large number of sites considered of low and medium heat flow. The high and very high geothermal gradient (Fig. 8b) and heat flow estimations (Fig. 9b), con-

sidered high heat flow sites, are located mainly in geothermal zones where convective heat transport occurs, as has already been shown in the works of Espinoza-Ojeda et al. (2017b) and Prol-Ledesma et al. (2018). The large amount of data in the updated heat flow database covers, alas unevenly, all the geologic provinces in México (see Fig. 1).

The realization of the updated geothermal gradient and heat flow map was enabled by the application of two interpolation methods. The reliability of the interpolation by IDW and EBK was measured through the correlation plots between the actual data values (heat flow and geothermal gradient) and the values estimated by each method (Fig. 10). In Figure 10, the R^2 is indicated for each analyzed case to identify the best interpolation method. From the correlation plots in Figure 10, it appears that the IDW method produced better interpolation results, with R^2 of 0.9605 and 0.9673, while EBK yielded R^2 of only 0.7935 and 0.8834 for heat flow and geothermal gradient, respectively. Thus, according to the results shown in Figure 10,

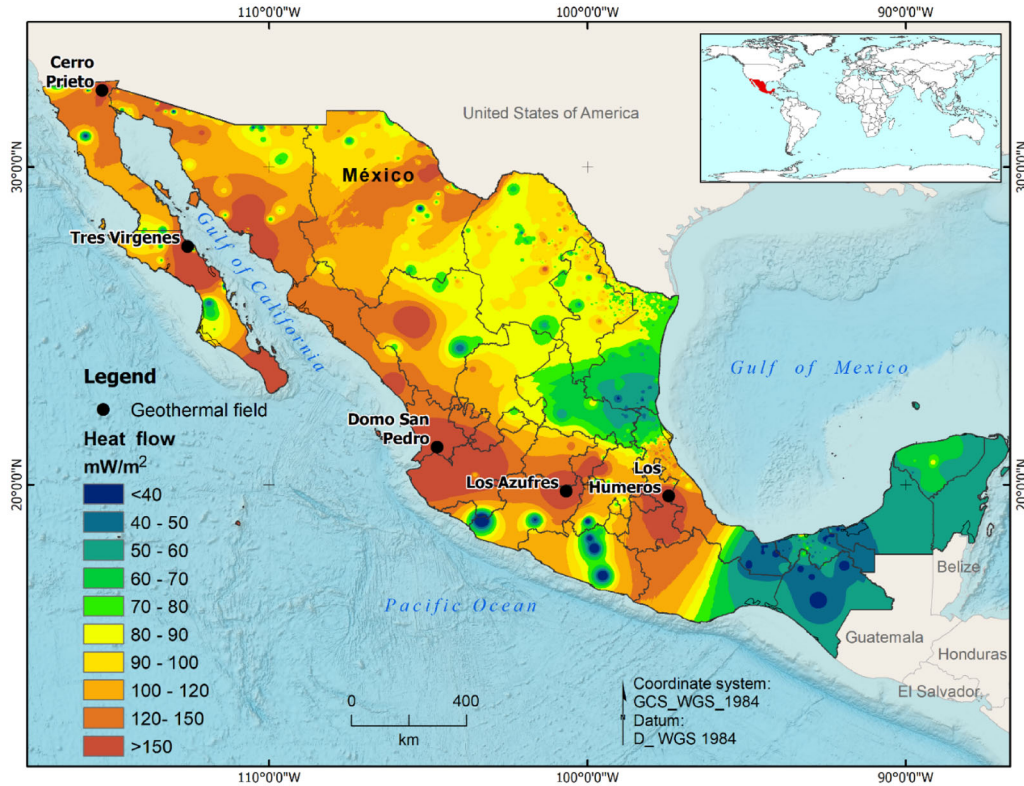


Figure 12. Continental heat flow map of México (updated: 2022). Locations of the Mexican geothermal fields (Cerro Prieto, Las Tres Vírgenes, Domo San Pedro, Los Azufres and Los Humeros) are shown as references of areas with known thermal anomalies.

the interpolation of all the available continental geothermal gradient and heat flow measurements in México was performed with the IDW method. Considering all the points within search distance, the weighting function *Inverse Distance to a Power* was used, and the selected power was 2. These parameters provided the best results in the evaluation; therefore, the model resolution of 500 m appears sufficient to resolve the continental trends.

The Mexican geothermal gradient map is described in Figure 11, where zones with geothermal gradient above the continental average (≈ 30 °C/km) can be observed. Excluding the current geothermal fields under exploitation, known as zones with thermal anomalies, several zones with increased continental-scale thermal regime can be found, providing extensive areas for regional exploration. These zones contain gradients of > 40 °C/km, as illustrated in central and northeastern México like “hot spot” anomalies. In northwestern México, large zones with gradients of > 45 °C/km were highlighted where interesting prospects may be located.

Lucazeau (2019) reported that the heat flow arithmetic mean varies from 62.4 to 68.4 mW/m^2 in the continental domain for oil data and non-oil data, respectively. These values clearly highlight the importance of high heat flow values that characterize large parts of México. The heat flow map (Fig. 12) shows anomalously high and very high heat flow values (≥ 200 mW/m^2) that are assumed to be representative of the TransMexican Volcanic Belt (center of México), among which Domo San Pedro, Los Azufres and Los Humeros geothermal fields are currently under exploitation, while other geothermal prospects such as Cerritos Colorados and Las Derumbadas are being evaluated. This thermal anomaly is related to local processes (e.g., volcanism and tectonics) and a significant convective component in the heat transfer. As a consequence, thousands of volcanic Middle Miocene to Holocene structures (some still active: ~ 5 Ma) and some intrusive bodies can be found (Ferrari et al., 2012) as well as active intraplate tectonic structures, resulting in magmatic intrusions as heat sources of the current

geothermal fields, and lastly also several geothermal prospects (Gutiérrez & Aumento, 1982; Jácome-Paz et al., 2019; Reyes-Orozco et al., 2019; Mazzoldi et al., 2020; Olvera-García et al., 2020a, b; Sourisseau et al., 2020).

In southern (e.g., Sierra Madre del Sur) and southeastern México (e.g., Southeast basin and Yucatan Peninsula), no geothermal resources have been prospected. That is because low heat flow values (≤ 50 mW/m²) are predominant in the back-arc region of the Middle America trench and local hydrothermal activity related with El Chichón and Tacaná active volcanoes is too restricted to increase the regional heat flow. The arc magmatism has reflected differences in the southern thermal structure due to the predicted cold slab-mantle interface temperatures, which are lower than one-half of the initial mantle temperature. Along the slab-mantle interface, underthrusting removes heat from the upper plate and interface temperatures decrease (e.g., Ziafos et al., 1985; Prol-Ledesma et al., 1989; Peacock, 2003; Manea et al., 2005; Minshull et al., 2005; van Keken & King, 2005; Currie & Hyndman, 2006). There are medium heat flow sites in southeastern México (>60 mW/m²) and, in the Yucatan Peninsula, some could be characterized as geopressurized resources associated with oil deposits (e.g., Southeast basin) (Shann, 2020); these local anomalies might have originated from a combination of factors like radiogenic activity in the crust and upper mantle, and the Chicxulub crater formation could raise the mantle lithosphere causing an increased surface heat flow (e.g., Flores-Márquez et al., 1999; Wilhelm et al., 2004; Șafanda et al., 2005; Espinosa-Cerdeña et al., 2016).

Zones with geothermal resources from medium to high heat flow are predominantly concentrated in northern México (>70 mW/m²). The tectonic province of the Sierra Madre Oriental and the Sabinas and Burgos basins is located in northeastern México. The thermal alterations observed in this territory are derived from processes of sedimentation and subsidence in a basin, i.e., thermal history of the sedimentary strata is perturbed during the development of the basin, which is directly related to the predominant conductive heat flow coming from deeper strata in most sedimentary basins, and also related to the increase in burial depth with time (Cuevas Lereee, 1985; Gray et al., 2001; Eguiluz-de Antuñano, 2009; Davison & Cunha, 2017). Some high heat flow sites that are widespread in the Sabinas and Burgos

basins (> 100 mW/m²) are related with recent intraplate volcanism (Aranda-Gómez et al., 2005).

In the case of central northern México, high heat flow isotherms (> 100 mW/m²) are predominant, even though some low heat flow areas (≤ 60 mW/m²) can be observed (Fig. 12). The development of the Gulf of California is the result of the cessation of subduction of the Farallon plate beneath North America when the Farallon plate was consumed, and the spreading centers collided with the North American plate (Larson et al., 1968; Moore & Buffington, 1968; Fletcher & Munguía, 2000; Ferrari et al., 2017). This event produced geologic activity described as volcanism and faulting (Angelier et al., 1981; Suarez-Vidal et al., 1991; Nourse et al., 1994; Mora-Klepeis & McDowell, 2004; Busby et al., 2020). The opening of the Gulf of California produced extensional tectonics in northwestern México, creating the southern extension of the Basin and Range tectonic province by normal faulting (Hamilton, 1987; Henry & Aranda-Gomez, 1992; Aranda-Gómez et al., 2000; Ferrari et al., 2013). Some models of continental extension indicate that the great variety of styles may reflect different thermal states during the initiation of rifting (Buck, 1991). The estimated high heat flow patterns could be similar to those of the southern Basin and Range and the Rio Grande rift (Decker & Smithson, 1975; Reiter et al., 1978; Smith & Jones, 1979; Mareschal & Bergantz, 1990; Lachenbruch et al., 1994; Wisian & Blackwell, 2004).

Finally, we observe evident variations from low to high heat flow isotherms predominate in northwestern México (Fig. 12). These are consistent with several studies that conclude that the regions around the Gulf of California (Baja California Peninsula and Sonora State) have many sites with possible significant geothermal potential, and some areas to be developed as geothermal projects (Campbell-Ramirez et al., 1993; Barragán et al., 2000, 2001; Quintero et al., 2005; Arango-Galván et al., 2015). Four regions can be considered the most remarkable according to their energy levels described in Figure 12: Guaymas, Sonora (> 150 mW/m²; adjacent to the Guaymas basin) (Williams et al., 1979; Prol-Ledesma, 1991; Almirudis et al., 2018); tip of the Baja California Peninsula (> 150 mW/m²) (López-Sánchez et al., 2006; Hernández-Morales & Wurl, 2017; Prol-Ledesma et al., 2021); areas close to the Tres Vírgenes geothermal field (> 150 mW/m²) (Prol-Ledesma et al., 2004; Villanueva-Estrada et al., 2012; Leal Acosta et al., 2013; Leal-Acosta &

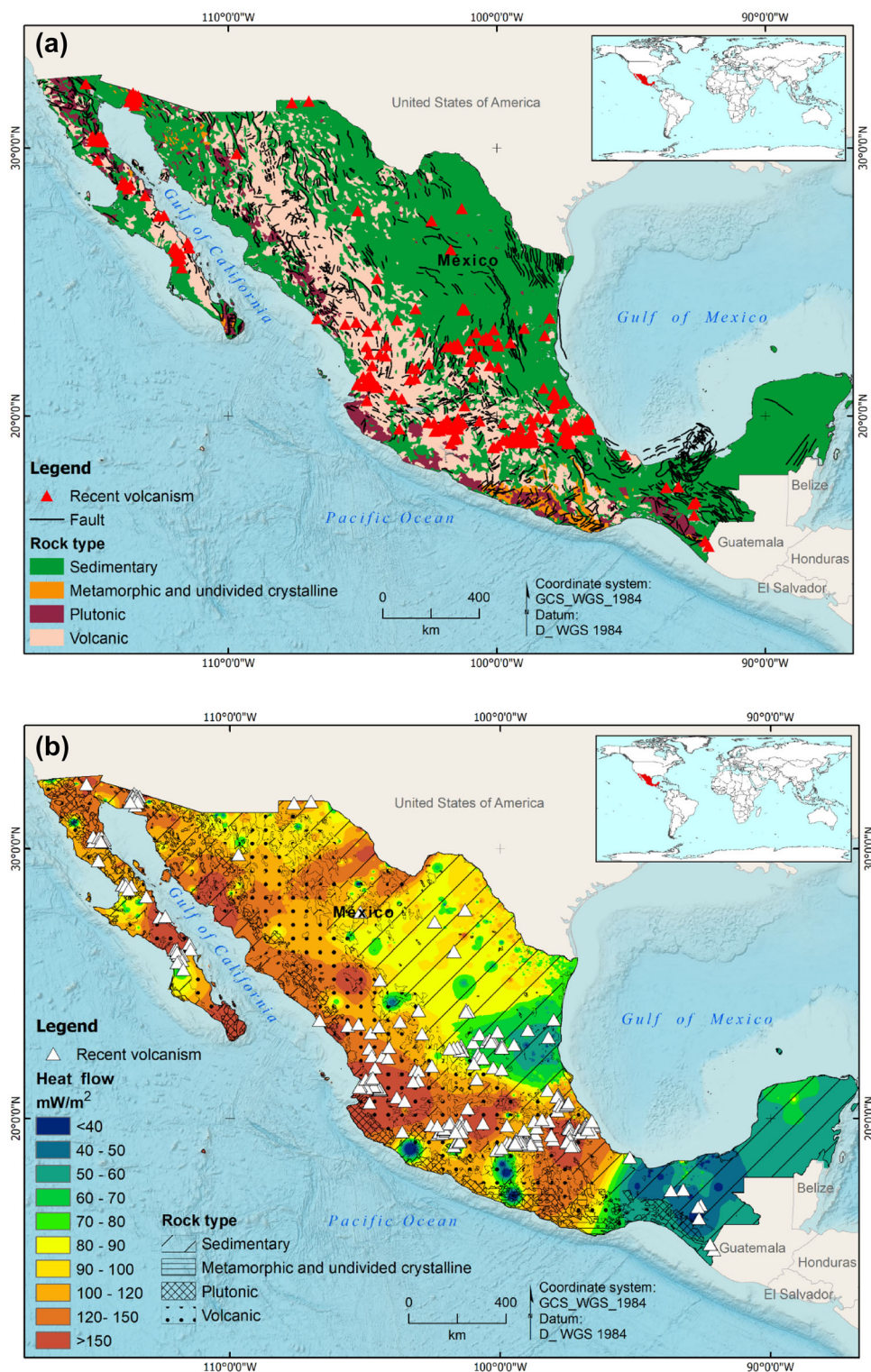


Figure 13. Geothermal plays in México: (a) regional geology, tectonics (Recent volcanism), and fault system; (b) correlation between regional geology and thermal regime (conduction dominated heat transport); and (c) correlation between regional fault system and thermal regime (conduction dominated heat transport).

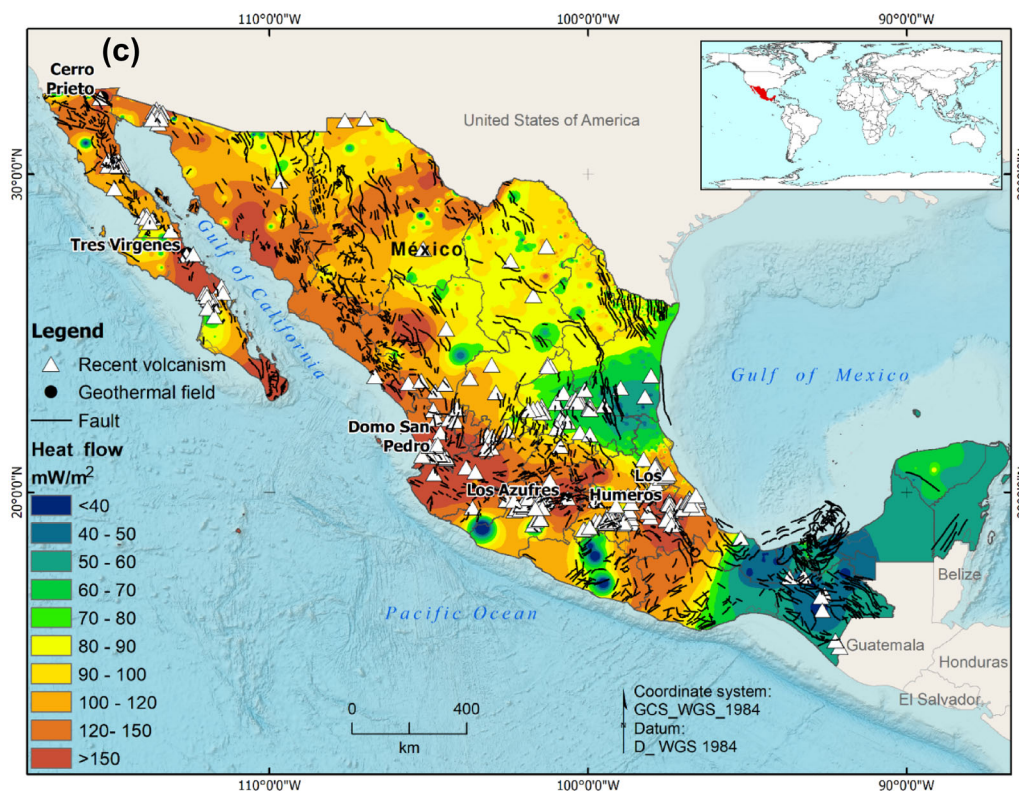


Figure 13. continued.

Prol-Ledesma, 2016; Sena-Lozoya et al., 2020; Hernández-Morales et al., 2021); the northern part of the Baja California Peninsula ($> 100 \text{ mW/m}^2$), from the Pacific coast to areas around Cerro Prieto and close to the Salton Through (Lee & Henyey, 1975; Vidal et al., 1978; 1981; Chavez, 1987; Reyes-Lopez et al., 1993; Elders, 1996; Beltran-Abaunza & Quintanilla-Montoya, 2001; Arango-Galván et al., 2011; González-García et al., 2018; Aguilar-Ojeda et al., 2021). These thermal anomalies could be attributed to hydrothermal convection phenomena related with structures produced by the development of the Gulf of California. Within naturally permeable structures, the presence of convective cells allows to generate temperature anomalies at economically interesting depths (e.g., Fig. 4: MEX0137). Recent studies showed that the presence of fluid in an abnormally permeable area is a factor that allows the development of a geothermal resource, from a natural geothermal heat flow (Guillou-Frottier et al., 2020; Duwiquet et al., 2020, 2021, 2022). As a side note, various studies have found that variation in continental heat flow is re-

lated to the age of the lithosphere (Polyak & Smirnov, 1968; Vitorello & Pollack, 1980). Nevertheless, the age of continents is more complicated to estimate than the oceanic lithosphere, as it involves an overlap of thermal processes (rifting or crustal extension, magmatic intrusions, erosion, etc.) (Sclater et al., 1981; Stein & Stein, 1992).

In this study, we focused on a reliable selection of deep boreholes with thermal data and analyzed their influence on the current heat flow database mostly using data from sedimentary basins, where heat flow is estimated mainly from depleted/exploration petroleum boreholes. This confirms that data from petroleum boreholes allow for improved statistical analysis, as high-quality estimates of geothermal gradients are achieved with greater depth and/or more temperature measurements (e.g., Figs. 6, 7). With increase in the number of heat flow sites within sedimentary basin types, thermal anomalies are better defined, as most high heat flow sites are located in active extensional areas (rifts) and the lowest values are found in coastal plain areas (along the coast of the Gulf of México,

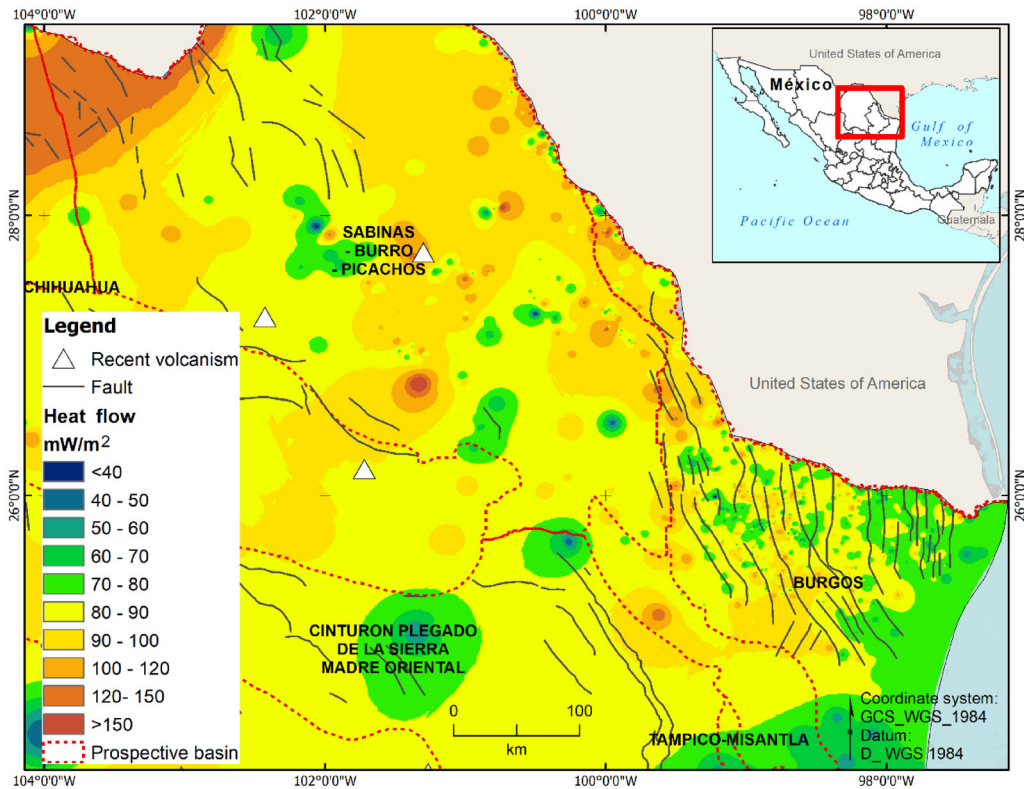


Figure 14. Geothermal plays in northeastern México (Sabinas and Burgos basins): correlation between thermal regime (conduction dominated heat transport) with regional tectonics (associated with volcanism intraplate) and fault system. Red dotted lines represent limits of the northeastern México basins.

excluding the Gulf coast central region that coincides with the TransMexican Volcanic Belt).

Although there are still large areas without available measurements, this had no negative effect on the statistics of the numerical prediction (interpolation), which showed the smooth variation in the thermal regime, e.g., the interpolation provided reliable heat flow estimates in the NW part of México because there are no significant variations in lithology of the region and the conductive heat transfer component is predominant. Unquestionably, the availability of more thermal data in those “gap” areas might improve the statistics for regional heat flow prediction. Figure 10 demonstrates that distinct choices of features can lead to quite different predictions even for regions without any constraining measurements.

The preceding discussions were the motivation for including the possible contribution of GPFA to this work. Figure 13 shows the geologic framework, which helps to describe the location of three different types of geothermal plays: regional geology to define sedimentary, metamorphic, plutonic and vol-

canic plays, and the main fault systems (Fig. 13a); correlation between thermal regime, recent volcanism (≤ 3 Ma) and play type (Fig. 13b); and correlation of thermal regime with the main fault systems (Fig. 13c) (Garrity & Soller, 2009; Padilla y Sánchez et al., 2013), and recent volcanism (≤ 3 Ma) (Duffield et al., 1984; Moran-Zenteno, 1986; Aranda-Gómez et al., 2000, 2005; Ferrari et al., 2005, 2007; Valdez Moreno et al., 2011; Global Volcanism Program, 2013; Macías & Arce, 2019; Prol-Ledesma & Morán-Zenteno, 2019).

The northeast of México was selected to analyze the application of the GPFA, where the Sabinas and Burgos basins are located; this area is characterized by sedimentary rock formations, few recent volcanisms, but with an outstanding regional fault system. According to the works by Aranda-Gómez et al. (2005), Valdez Moreno et al (2011) and Padilla y Sánchez et al. (2013), it was possible to characterize the intraplate volcanism, regional geology and fault systems in Figure 14. From Figure 14, we observe that the relative high heat flow values (80–120 mW/m^2) are directly linked to recent volcanism in

the Sabinas basin (Aranda-Gómez et al., 2005; Valdez Moreno et al., 2011) and to the regional fault system of the Burgos basin (Eguiluz-de Antuñano, 2009; Padilla y Sánchez et al., 2013). Some of the intraplate volcanism is aligned along regional normal faults, suggesting that magma could have ascended through regional faults (Aranda-Gómez et al., 2005; Valdez Moreno et al., 2011). The GPFA application to the geological and heat flow data provides the highest likelihood of success in the search for prospects to exploit geothermal resources, even when data are sparse or incomplete. Additionally, the GPFA aids in the discovery of new geothermal resources. Therefore, the application of the GPFA to new heat flow data and the integration described in Figure 14 revealed that oil/gas producing areas in northeastern México can be considered as prospective zones with medium- to high-enthalpy geothermal resources.

While the heat flow maps published by Prol-Ledesma et al. (2018) and Prol-Ledesma and Morán-Zenteno (2019) show no differences, and although the analysis and description of the results were carried out for different purposes, the integration of Curie temperature data and hydrothermal manifestations data, together with direct measurements from the boreholes, might yield consistent maps for regional geothermal prospecting. The outcome, presented here, could be classified as a very precise map with values obtained only from direct thermal measurements in the boreholes. Therefore, this work provides almost 4,000 additional data to better define low, medium and high heat flow isotherms areas. Besides, the previously compiled and newly estimated thermal data are important contributions for discovering unknown low- and medium-enthalpy sites and provides the basis for the application of GPFA, thereby increasing the probability to identify new geothermal prospects. In addition, this work has a direct impact on both geothermal and petroleum industries, considering that most of the evaluated sites are petroleum boreholes and support the proposal of simultaneous geothermal/oil resources development. Therefore, it is a synergy of petroleum and geothermal industry.

CONCLUSIONS

The update of the Mexican heat flow database consists in the integration of 3,888 new data (3,871 continental and 17 offshore), the largest compilation

carried out to date. This work represents a noteworthy increased number in the compilation of published and new geothermal gradients and heat flow measurements in México. The combination of these data improved the corresponding contouring maps. The updated geothermal gradient and heat flow database will be indispensable to carry out rigorous estimates of the heat reserves stored in the crust. The thermal anomalies reported in this work allow to locate promising areas for exploitation and direct use of geothermal energy. The increase in valuable data in the heat flow database can be combined with GPFA to discover new geothermal resources; the new prospects can be cataloged in an alternative way according to their geological characteristics and thermal regime. From the results, the predominant interval values for geothermal gradient and heat flow were 25–55 °C/km and 40–140 mW/m², respectively. In the north and central east coast of Mexico, there are large areas with wide variations in heat flow, from low to high values, which are an energetic attraction to be characterized by geothermal prospecting. In addition, the results obtained confirm that Mexico has great geothermal potential to be exploited through direct uses. As future work, constant update and analysis of geothermal gradient and heat flow measurements are necessary to reveal low-, medium- and high-enthalpy resources in large areas that remain uncharted.

ACKNOWLEDGMENTS

The authors would like to express gratitude to Comisión Federal de Electricidad (CFE) and Petróleos Mexicanos (PEMEX) for providing data. This work received support from projects: PN2015-01-388 “Aprovechamiento de pozos petroleros abandonados/inoperantes como fuente sustentable de energía para sistemas híbridos Geotermia/Concentrador Solar,” from the national program Proyectos de Desarrollo Científico para Atender Problemas Nacionales 2015 (CONACYT); CeMIE-Geo P-01 “Mapas de Gradiente Geotérmico y Flujo de Calor para la República Mexicana.” Thanks to the technicians of INICIT-UMSNH: M.C. Alejandro García Casillas† and M.C. Nancy Magaña García, for their help and support during the collection and processing of thermal data. We are also grateful to Dr. Duwiquet Hugo, M.Sc. Dušan Rajver and two anonymous reviewers for their helpful comments on

an earlier version of the paper. Revision and copy editing of the final draft were carried out by Ambar Geerts Zapién.

FUNDING

Financial support by CONACyT, through projects number PN2015-01–388 and CeMIE-Geo P-01.

AVAILABILITY OF DATA AND MATERIALS

https://github.com/omespinozaojeda/Mexico_HF_database.git.

DECLARATIONS

Conflict of Interest The authors declare that they have no conflicts of interests or known competing financial interests.

REFERENCES

- Aguilar-Ojeda, J. A., Campos-Gaytán, J. R., Villela, A., Herrera-Oliva, C. S., Ramírez-Hernandez, J., & Kretzschmar, T. G. (2021). Understanding hydrothermal behavior of the Manadero geothermal system, Ensenada, Baja California, Mexico. *Geothermics*, 89, 101985.
- Almaguer, J., Lopez-Loera, H., Macias, J. L., Saucedo, R., Yutsis, V., & Guevara, R. (2020). Geophysical modeling of La Primavera caldera and its relation to volcanology activity based on 3D susceptibility inversion and potential data analysis. *Journal of Volcanology and Geothermal Research*, 393, 106556.
- Almirudis, E., Santoyo, E., Guevara, M., Paz-Moreno, F., & Portugal, E. (2018). Chemical and isotopic signatures of hot springs from east-central Sonora State, Mexico: a new prospection survey of promissory low-to-medium temperature geothermal systems. *Revista Mexicana de Ciencias Geológicas*, 35(2), 116–141.
- American Association of Petroleum Geologists (AAPG). (1976). *Basic data file from AAPG geothermal survey of North America*. University of Oklahoma.
- Angelier, J., Colletta, B., Chorowicz, J., Ortlieb, L., & Rangin, C. (1981). Fault tectonics of the Baja California Peninsula and the opening of the Sea of Cortez, Mexico. *Journal of Structural Geology*, 3(4), 347–357.
- Aranda-Gómez, J. J., Henry, C. D., & Luhr, J. F. (2000). Evolución tectonomagmática post-paleocénica de la Sierra Madre Occidental y de la porción meridional de la provincia tectónica de Cuencas y Sierras, México. *Boletín de la Sociedad Geológica Mexicana*, 8, 59–71.
- Aranda-Gómez, J. J., Luhr, J. F., Housh, T. B., Valdez-Moreno, G., & Chávez-Cabello, G. (2005). El volcanismo tipo intraplaca del Cenozoico tardío en el centro y norte de México: Una revisión. *Boletín de la Sociedad Geológica Mexicana*, LVII(3), 187–225.
- Arango-Galván, C., Prol-Ledesma, R. M., Flores-Márquez, E. L., Canet, C., & Villanueva, R. E. (2011). Shallow submarine and subaerial, low-enthalpy hydrothermal manifestations in Punta Banda, Baja California, Mexico: Geophysical and geochemical characterization. *Geothermics*, 40(2), 102–111.
- Arango-Galván, C., Prol-Ledesma, R. M., & Torres-Vera, M. A. (2015). Geothermal prospects in the Baja California Peninsula. *Geothermics*, 55, 39–57.
- Avellán, D. R., Macías, J. L., Laver, P. W., Cisneros, G., Sánchez-Núñez, J. M., Gómez-Vasconcelos, M. G., Pola, A., Sosa-Ceballos, G., García-Tenorio, F., Reyes Agustín, G., Osorio-Ocampo, S., García-Sánchez, L., Mendiola, I. F., Marti, J., López-Loera, H., & Benowitz, J. (2018). Geology of the late Pliocene—Pleistocene Aocolul caldera complex, eastern Trans-Mexican Volcanic Belt (México). *Journal of Maps*, 15(2), 8–18.
- Báncora, C., & Prol-Ledesma, R. M. (2008). Geothermal exploration using remote sensing in the south of Baja California Sur, Mexico. In *Proceedings of the AIP conference proceedings* (pp. 180–188). <https://doi.org/10.1063/1.2937285>.
- Barragán, R. M., Portugal, E., Birkle, P., Arellano, V. M., & Alvarez, J. (2000). Geochemical survey of medium temperature geothermal resources in the NW zone of México. In *Proceedings of the 21th PNOC geothermal conference, Manila, Filipinas* (pp. 233–240).
- Barragán, R. M., Birkle, P., Portugal, E., Arellano, V. M., & Alvarez, J. (2001). Geochemical survey of medium temperature geothermal resources from Baja California and Sonora, Mexico. *Journal of Volcanology and Geothermal Research*, 110, 101–119.
- Bartier, P. M., & Keller, P. (1996). Multivariate interpolation to incorporate thematic surface data using inverse distance weighting (IDW). *Computers & Geosciences*, 22(7), 795–799.
- Becker, K. (1981). *Heat flow studies of spreading center hydrothermal processes* (Ph.D. dissertation, Scripps Institution of Oceanography, University of California, San Diego, California), 149p.
- Becker, K., & Fisher, A. T. (1991). A brief review of heat-flow studies in the Guaymas Basin, Gulf of California. In J. P. Dauphin & B. R. Simoneit (Eds.), *The Gulf and Peninsular Province of the Californias* (pp. 709–720). American Association of Petroleum Geologists.
- Beltran-Abauza, J. M., & Quintanilla-Montoya, A. L. (2001). Calculated heat flow for the Ensenada region, Baja California. *Mexico. Ciencias Marinas*, 27(4), 619–634.
- Bevington, P. R., & Robinson, D. (2003). *Data reduction and error analysis for the physical sciences* (3rd ed., p. 320pp). McGraw Hill Higher Education.
- Blackwell, D.D., & Richards, M. (2004). Geothermal map of North America. In *American Association of Petroleum Geologist (AAPG)*, 1 sheet, scale 1:6,500,000.
- Buck, W. R. (1991). Modes of lithospheric extension. *Journal of Geophysical Research*, 96, 20161–20178.
- Bullard, E. C. (1939). Heat flow in South Africa. *Proceedings of the Royal Society of London Series A, Mathematical and Physical Sciences*, 173, 474–502.
- Busby, C., Graettinger, A., López Martínez, M., Medynski, S., Niemi, T., Andrews, C., Bowman, E., Gutierrez, E. P., Henry, M., Lodes, E., Ojeda, J., Rice, J., Andrews, G., & Brown, S. (2020). Volcanic record of the arc-to-rift transition onshore of the Guaymas basin in the Santa Rosalia area, Gulf of California, Baja California. *Geosphere*, 16(4), 1012–1041.
- Campbell-Ramirez, H., Elders, W. A., Reyes-Lopez, J., Ramirez-Hernandez, J., Vega-Aguilar, M., & Carreon-Diazconti, C. (1993). Potential for direct-use of geothermal energy for the Mexicali valley, Baja California, Mexico. *Geothermal Resources Council Transactions*, 17, 3–9.
- Campos-Enríquez, J. O., Espinosa-Cardena, J. M., & Oksum, E. (2019). Subduction control on the curie isotherm around the

- Pacific-North America plate boundary in northwestern Mexico (Gulf of California). Preliminary results. *Journal of Volcanology and Geothermal Research*, 375, 1–17.
- Chavez, R. E. (1987). An integrated geophysical study of the geothermal field of Tule Chek, B.C., Mexico. *Geothermics*, 16(5–6), 529–538.
- Crowell, A. M., Ochsner, A. T., & Gosnold, W. (2012). Correcting bottom-hole temperatures in the Denver Basin: Colorado and Nebraska. *Geothermal Resources Council Transactions*, 36, 201–206.
- Cuevas Leree, J. A. (1985). *Analysis of subsidence and thermal history in the Sabinas Basin, northeastern Mexico* (University of Arizona. Master thesis), 81pp. <http://hdl.handle.net/10150/558018>.
- Currie, C. A., & Hyndman, R. D. (2006). The thermal structure of subduction zone back arcs. *Journal of Geophysical Research*, 111(B8), B08404.
- Davison, I., & Cunha, T. A. (2017). Allochthonous salt sheet growth: Thermal implications for source rock maturation in the deepwater Burgos Basin and Perdido Fold Belt, Mexico. *Interpretation*, 5(1), T11–T21.
- Decker, E. R., & Smithson, S. B. (1975). Heat flow and gravity interpretation across the Rio Grande rift in southern New Mexico and west Texas. *Journal of Geophysical Research*, 80(17), 2542–2552.
- Deming, D. (1989). Application of bottom-hole temperature corrections in geothermal studies. *Geothermics*, 18(5–6), 775–786.
- Dobson, P. F. (2016). A review of exploration methods for discovering hidden geothermal systems. *Geothermal Resources Council Transactions*, 40, 695–706.
- Duffield, W. A., Tilling, R. A., & Canul, R. (1984). Geology of El Chichon volcano, Chiapas, Mexico. *Journal of Volcanology and Geothermal Research*, 20(1–2), 117–132.
- Duwiguet, H., Guillou-Frottier, L., Arbaret, L., Guillon, T., Bellanger, M., & Heap, M. J. (2020). Crustal Fault Zone: New geothermal reservoir? Structural dataset and preliminary 3D TH(M) modelling of the Pontgibaud fault zone (French Massif Central). In *Proceedings of the 45th workshop on geothermal reservoir engineering, Stanford University, Stanford, California, February 10–12* (pp. 1–11).
- Duwiguet, H., Guillou-Frottier, L., Arbaret, L., Bellanger, M., Guillon, T., & Heap, M. J. (2021). Crustal Fault Zones (CFZ) as geothermal power systems: A preliminary 3D THM model constrained by a multidisciplinary approach. *Geofluids*, 2021, 8855632.
- Duwiguet, H., Magri, F., Lopez, S., Guillon, T., Arbaret, L., Bellanger, M., & Guillou-Frottier, L. (2022). Tectonic regime as a control factor for Crustal Fault Zone (CFZ) geothermal reservoir in an amagmatic system: A 3D dynamic numerical modeling approach. *Natural Resources Research*, 31, 3155–3172.
- Eguiluz-de Antuñano, S. (2009). The Yegua Formation: Gas play in the Burgos Basin, Mexico. In C. Bartolini & J. R. Román Ramos (Eds.), *Petroleum systems in the southern Gulf of Mexico* (pp. 49–77). The American Association of Petroleum Geologists. <https://doi.org/10.1306/13191077M902621>.
- Elders, W. A. (1996). Direct use potential of the Tule Chek geothermal area, B.C., Mexico. *Geothermal Resources Council Transactions*, 20, 73–80.
- Epp, D., Grim, P. J., & Langseth, M. G. J. (1970). Heat flow in the Caribbean and Gulf of Mexico. *Journal of Geophysical Research*, 75(29), 5655–5669.
- Erickson, A. J., Helsey, C. E., & Simmons, G. (1972). Heat flow and continuous seismic profiles in the Cayman Trough and Yucatan basin. *Geological Society of America Bulletin*, 83(5), 1241–1260.
- Espinosa-Cerdeña, J. M., Campos-Enríquez, J. O., & Unsworth, M. (2016). Heat flow pattern at the Chicxulub impact crater, northern Yucatan, Mexico. *Journal of Volcanology and Geothermal Research*, 311, 135–149.
- Espinosa-Ojeda, O. M., Prol-Ledesma, R. M., & Iglesias, E. R. (2017a). Continental heat flow data update for México—Constructing a reliable and accurate heat flow map. In: *Proceedings of the 42nd workshop on geothermal reservoir engineering, Stanford University, Stanford, California* (pp. 1–14).
- Espinosa-Ojeda, O. M., Prol-Ledesma, R. M., Iglesias, E. R., & Figueroa-Soto, A. (2017b). Update and review of heat flow measurements in Mexico. *Energy*, 121C, 466–479.
- Faulds, J. E., & Hinz, N. H. (2015). Favorable tectonic and structural settings of geothermal systems in the Great Basin region, western USA: Proxies for discovering blind geothermal systems. In *Proceedings of the world geothermal congress 2015, Melbourne, Australia, 19–25 April* (pp. 1–6).
- Ferrari, L., Tagami, T., Eguchi, M., Orozco-Esquivel, M. T., Petrone, C. M., Jacobo-Albarrán, J., & López-Martínez, M. (2005). Geology, geochronology and tectonic setting of late Cenozoic volcanism along the southwestern Gulf of Mexico: The Eastern Alkaline Province revisited. *Journal of Volcanology and Geothermal Research*, 146(4), 284–306.
- Ferrari, L., Valencia-Moreno, M., & Bryan, S. (2007). Magmatism and tectonics of the Sierra Madre Occidental and its relation with the evolution of the western margin of North America. *Geological Society of America Special Paper*, 422, 1–39.
- Ferrari, L., Orozco-Esquivel, T., Manea, V., & Manea, M. (2012). The dynamic history of the Trans-Mexican Volcanic Belt and the Mexico subduction zone. *Tectonophysics*, 522–523, 122–149.
- Ferrari, L., López-Martínez, M., Orozco-Esquivel, T., Bryan, S. E., Duque-Trujillo, J., Lonsdale, P., & Solari, L. (2013). Late Oligocene to middle Miocene rifting and synextensional magmatism in the southwestern Sierra Madre Occidental, Mexico: The beginning of the Gulf of California rift. *Geosphere*, 9(5), 1–40.
- Ferrari, L., Bonini, M., & Martin-Barajas, A. (2017). From continental to oceanic rifting in the Gulf of California. *Tectonophysics*, 719–720, 1–3.
- Fisher, A. T., Giambalvo, E., Sclater, J., Kastner, M., Ransom, B., Weinstein, Y., & Lonsdale, P. (2001). Heat flow, sediment and pore fluid chemistry, and hydrothermal circulation on the east flank of Alarcon Ridge, Gulf of California. *Earth and Planetary Science Letters*, 188, 521–534.
- Fletcher, J. M., & Munguía, L. (2000). Active continental rifting in southern Baja California, Mexico: Implications for plate motion partitioning and the transition to seafloor spreading in the Gulf of California. *Tectonics*, 19(6), 1107–1123.
- Flores-Márquez, E. L., Chávez-Segura, R., Campos-Enríquez, O., & Pilkington, M. (1999). Preliminary 3-D structural model from the Chicxulub impact crater and its implications in the actual geothermal regime. *Trends in Heat, Mass & Momentum Transfer*, 5, 19–40.
- Förster, A., & Merriam, D. F. (1995). A bottom-hole temperature analysis in the American Midcontinent (Kansas): Implications to the applicability of BHTs in geothermal studies. In *Proceedings of the World Geothermal Congress, Florence, Italy* (pp. 777–782).
- Förster, A., Merriam, D. F., & Davis, J. C. (1995). Statistical analysis of some bottom-hole temperature (BHT) correction factors for the Cherokee Basin, southeastern Kansas. In *Transactions of the 1995 AAPG mid-continent section meeting, Tulsa, Oklahoma*.
- Fuchs, S., Balling, N., & Mathiesen, A. (2020). Deep basin temperature and heat-flow field in Denmark—New insights from borehole analysis and 3D geothermal modelling. *Geothermics*, 83, 101722.

- Fulton, P. M., & Saffer, D. M. (2009). Effect of thermal refraction on heat flow near the San Andreas Fault, Parkfield, California. *Journal of Geophysical Research*, 114(B06408), 1–12.
- Garrity, C.P., & Soller, D.R. (2009). Database of the Geologic Map of North America; adapted from the map by J.C. Reed, Jr. and others. U.S. Geological Survey Data Series 424. [h <https://pubs.usgs.gov/ds/424/>]. <https://doi.org/10.3133/ds424>.
- Global Volcanism Program (2013). Volcanoes of the World, v. 4.10.0 (14 May 2021). In Venzke, E. (Ed.), *Smithsonian Institution*. Retrieved May 20, 2021, from <https://volcano.si.edu/>.
- González-García, H., Prol-Ledesma, R. M., Amaro-Rodiles, F., & Arango-Galván, C. (2018). Financial and technical feasibility study of the low enthalpy geothermal system “La Jolla”, Baja California Mexico. In *Proceedings of the 43rd Workshop on Geothermal Reservoir Engineering, Stanford University, Stanford, California, February 12–14* (pp. 1–9).
- Gray, G. G., Pottorf, R. J., Yurewicz, D. A., Mahon, K. I., Pevear, D. R., & Chuchla, R. J. (2001). Thermal and chronological record of Syn- to Post-Laramide Burial and Exhumation, Sierra Madre Oriental, Mexico. In C. Bartolini, R. T. Buffler, & A. Cantú-Chapa (Eds.), *The Western Gulf of Mexico Basin: Tectonics, sedimentary basins, and petroleum systems*. American Association of Petroleum Geologists. <https://doi.org/10.1306/M75768C7>.
- Guerrero-Martínez, F. J., Prol-Ledesma, R. M., Carrillo-de la Cruz, J.-L., Rodríguez-Díaz, A. A., & González-Romo, I. A. (2020). A three-dimensional temperature model of the *Aco-culco caldera* complex, Puebla, Mexico, from the Curie isotherm as a boundary condition. *Geothermics*, 86, 101794.
- Guillou-Frottier, L., Duwiquet, H., Launay, G., Taillefer, A., Roche, V., & Link, G. (2020). On the morphology and amplitude of 2D and 3D thermal anomalies induced by buoyancy-driven flow within and around fault zones. *Solid Earth*, 11(4), 1571–1595.
- Gutiérrez, A., & Aumento, F. (1982). The Los Azufres, Michoacan, Mexico, geothermal field. *Journal of Hydrology*, 56, 137–162.
- Gutiérrez-Negrín, L. C. A. (2015). Mexican geothermal plays. In *Proceedings of the World Geothermal Congress 2015, Melbourne, Australia, 19–25 April* (pp. 1–9).
- Gutiérrez-Negrín, L. C. A., Beardmore, G., Garduño-Monroy, V. H., Espinoza-Ojeda, O. M., Almanza-Álvarez, S., Antriasian, A., & Egan, S. (2020). Field trial of a surface heat flow probe at the Cuitzeo Lake geothermal zone, Mexico. In *Proceedings of the World Geothermal Congress 2020+1, Reykjavik, Iceland, April–October 2021* (pp. 1–10).
- Hamilton, W. (1987). Crustal extension in the Basin and Range Province, southwestern United States. *Geological Society, London, Special Publications*, 28, 155–176.
- Henry, C. D., & Aranda-Gomez, J. J. (1992). The real southern Basin and Range: Mid- to late Cenozoic extension in Mexico. *Geology*, 20(8), 701–704.
- Heney, T. L., & Bischoff, J. L. (1973). Tectonic elements of the northern part of the Gulf of California. *Geological Society of America Bulletin*, 84(1), 315–330.
- Hernández-Morales, P., & Wurl, J. (2017). Hydrogeochemical characterization of the thermal springs in northeastern of Los Cabos Block, Baja California Sur. *México. Environmental Science and Pollution Research*, 24(15), 13184–13202.
- Hernández-Morales, P., Wurl, J., Green-Ruiz, C., & Morata, D. (2021). Hydrogeochemical characterization as a tool to recognize “Masked Geothermal Waters” in Bahía Concepción. *Mexico. Resources*, 10(23), 1–24.
- Iglesias, E. R., Torres, R. J., Martínez-Estrella, I., & Reyes-Picasso, N. (2015). Summary of the 2014 assessment of medium- to low-temperature Mexican geothermal resources. In *Proceedings of the World Geothermal Congress 2015, Melbourne, Australia*, 1–7.
- Iglesias, E. R., Torres, R. J., Martínez-Estrella, J. I., Lira-Ar-güello, R., Paredes-Soberanes, A., Reyes-Picasso, N., Prol, R. M., Espinoza-Ojeda, O. M., López-Blanco, S., & González-Reyes, I. (2016). Potencial teórico SGM en los afloramientos del basamento en México. *Geotermia, Revista Mexicana de Geoenergía*, 29(2), 6–17.
- Instituto Nacional de Estadística y Geografía (INEGI). (2021). [h <https://www.inegi.org.mx/>](https://www.inegi.org.mx/).
- Jácome-Paz, M. P., Pérez-Zárate, D., Prol-Ledesma, R. M., Rodríguez-Díaz, A. A., Estrada-Murillo, A. M., González-Romo, I. A., & Magaña-Torres, E. (2019). Two new geothermal prospects in the Mexican Volcanic Belt: La Escalera and Agua Caliente—Tzitzio geothermal springs, Michoacán, México. *Geothermics*, 80, 44–55.
- Jobmann, M., & Clauser, C. (1994). Heat advection versus conduction at the KTB: Possible reasons for vertical variations in heat-flow density. *Geophysical Journal International*, 119(1), 44–68.
- Khutorskoy, M. D., Fernandez, R., Kononov, V. I., Polyak, B. G., Matveev, V. G., & Rot, A. A. (1990). Heat flow through the sea bottom around the Yucatan Peninsula. *Journal of Geophysical Research*, 95(B2), 1223–1237.
- Lachenbruch, A. H., Sass, J. H., & Morgan, P. (1994). Thermal regime of the southern Basin and Range Province: 2. Implications of heat flow for regional extension and metamorphic core complex. *Journal of Geophysical Research*, 99(B11), 22121–22133.
- Landa-Arreguín, J. F. A., Villanueva-Estrada, R. E., Rodríguez-Díaz, A. A., Morales-Arredondo, J. I., Rocha-Miller, R., & Alfonso, P. (2021). Evidence of a new geothermal prospect in the Northern-Central trans-Mexican volcanic belt: Rancho Nuevo, Guanajuato. *Mexico. Journal of Iberian Geology*, 47(4), 713–732.
- Larson, R. L., Menard, H. W., & Smith, S. M. (1968). Gulf of California: A result of ocean-floor spreading and transform faulting. *Science*, 161(3843), 781–784.
- Lawver, L. A., Sclater, J. G., Henyey, T. L., & Rogers, J. (1973). Heat flow measurements in the southern portion of the Gulf of California. *Earth and Planetary Science Letters*, 12(2), 198–208.
- Lawver, L. A., Williams, D. L., & Von Herzen, R. P. (1975). A major geothermal anomaly in the Gulf of California. *Nature*, 257, 23–28.
- Lawver, L. A., & Williams, D. L. (1979). Heat flow in the central Gulf of California. *Journal of Geophysical Research*, 84(B7), 3465–3478.
- Leal Acosta, M. L., Shumilin, E., & Mirlean, N. (2013). Sediment geochemistry of marine shallow-water hydrothermal vents in Mapachitos, bahía Concepción, Baja California peninsula. *Mexico. Revista Mexicana de Ciencias Geológicas*, 30(1), 233–245.
- Leal-Acosta, M. L., & Prol-Ledesma, R. M. (2016). Caracterización geoquímica de las manifestaciones termales intermareales de Bahía Concepción en la Península de Baja California. *Boletín de la Sociedad Geológica Mexicana*, 68(3), 395–407.
- Lee, T.-C., & Henyey, T. L. (1975). Heat flow through the southern California borderland. *Journal of Geophysical Research*, 80(26), 3733–3743.
- Lonsdale, P., & Becker, K. (1985). Hydrothermal plumes, hot springs, and conductive heat flow in the Southern Trough of Guaymas Basin. *Earth and Planetary Science Letters*, 73(2), 211–225.
- López-Sánchez, A., Bâncora-Alsina, C., Prol-Ledesma, R. M., & Hiriart, G. (2006). A new geothermal resource in Los Cabos, Baja California Sur, Mexico. In *Proceedings of the 28th New Zealand Geothermal Workshop, New Zealand*, 1–6.

- Lucazeau, F. (2019). Analysis and mapping of an updated terrestrial heat flow dataset. *Geochemistry, Geophysics, Geosystems*, 20(8), 4001–4024.
- Macías, J. L., & Arce, J. L. (2019). Volcanic activity in Mexico during the Holocene. In N. Torrescano-Valle (Ed.), *The Holocene and anthropocene environmental history of Mexico—A paleoecological approach on Mesoamerica* (pp. 129–170). Springer.
- Manea, V. C., Manea, M., Kostoglodov, V., & Sewell, G. (2005). Thermo-mechanical model of the mantle wedge in Central Mexican subduction zone and a blob tracing approach for the magma transport. *Physics of the Earth and Planetary Interiors*, 149(1), 165–186.
- Mareschal, J. C., & George, B. (1990). Constraints on thermal models of the Basin and Range province. *Tectonophysics*, 174(1–2), 137–146.
- Mazzoldi, A., Garduño-Monroy, V. H., Gómez Cortes, J. J., & Guevara Alday, J. A. (2020). Geophysics for geothermal exploration. Directional-derivatives-based computational filters applied to geomagnetic data at Lake Cuitzeo. *Mexico. Geofísica Internacional*, 59(2), 105–135.
- Miller, J. C., & Miller, J. N. (2000). *Statistics and chemometrics for analytical chemistry* (4th ed.). Prentice-Hall.
- Minshull, T. A., Bartolomé, R., Byrne, S., & Dañoibeitia, J. (2005). Low heat flow from young oceanic lithosphere at the Middle America Trench off Mexico. *Earth and Planetary Science Letters*, 239(1–2), 33–41.
- Moeck, I. S. (2014). Catalog of geothermal play types based on geologic controls. *Renewable and Sustainable Energy Reviews*, 37, 867–882.
- Moeck, I. S., Beardsmore, G., & Harvey, C. C. (2015). Cataloging worldwide developed geothermal systems by geothermal play type. In *Proceedings of the world geothermal congress 2015, Melbourne, Australia, 19–25 April* (pp. 1–9).
- Moore, D. G., & Buffington, E. C. (1968). Transform faulting growth of the Gulf of California since the late Pliocene. *Science*, 161(3847), 1238–1241.
- Mora-Klepeis, G., & McDowell, F. W. (2004). Late Miocene calc-alkalic volcanism in northwestern Mexico: An expression of rift or subduction-related magmatism? *Journal of South American Earth Sciences*, 17(4), 297–310.
- Moran-Zenteno, D. J. (1986). Breve revisión sobre la evolución tectónica de México. *Geofísica Internacional*, 25(1), 9–38.
- Nagihara, S., Sclater, J. G., Phillips, J. D., Behrens, E. W., Lewis, T., Lawver, L. A., Nakamura, Y., Garcia-Abdeslem, J., & Maxwell, A. E. (1996). Heat flow in the western abyssal plain of the Gulf of Mexico: Implications for thermal evolution of the old oceanic lithosphere. *Journal of Geophysical Research*, 101(B2), 2895–2913.
- Neumann, F., Negrete-Aranda, R., Harris, R. N., Contreras, J., Sclater, J. G., & González-Fernández, A. (2017). Systematic heat flow measurements across the Wagner Basin, northern Gulf of California. *Earth and Planetary Science Letters*, 479, 340–353.
- Negrete-Aranda, R., Neumann, F., Contreras, J., Harris, R. N., Spelz, R. M., Zierenberg, R., & Caress, D. W. (2022). Transport of heat by hydrothermal circulation in a young rift setting: Observations from the Auka and JaichMaa Ja'ag' vent field in the Pescadero Basin, Southern Gulf of California. *Journal of Geophysical Research: Solid Earth*, 126, e2021JB022300.
- Norden, B., Förster, A., Behrends, K., Krause, K., Stecken, L., & Meyer, R. (2012). Geological 3-D model of the larger Altsalzswedel area, Germany, for temperature prognosis and reservoir simulation. *Environmental Earth Sciences*, 67(2), 511–526.
- Nourse, J. A., Anderson, T. H., & Silver, L. T. (1994). Tertiary metamorphic core complexes in Sonora, northwestern Mexico. *Tectonics*, 13(5), 1161–1182.
- Olvera-García, E., Garduño-Monroy, V. H., Liotta, D., Brogi, A., Bermejo-Santoyo, G., & Guevara-Alday, J. A. (2020a). Neogene-Quaternary normal and transfer faults controlling deep-seated geothermal systems: The case of San Agustín del Maíz (central Trans-Mexican Volcanic Belt, México). *Geothermics*, 86, 101791.
- Olvera-García, E., Garduño-Monroy, V. H., Ostrooumov, M., Gaspar-Patarroyo, T. L., & Nájera-Blas, S. M. (2020b). Structural control on hydrothermal upwelling in the Ixtlán de los Hervores geothermal area, Mexico. *Journal of Volcanology and Geothermal Research*, 399, 106888.
- Padilla y Sánchez, R. J., Domínguez Trejo, I., López Azcárraga, A. G., Mota Nieto, J., Fuentes Menes, A.O., Rosique Naranjo, F., Germán Castelán, E. A., & Campos Arriola, S. E. (2013). National Autonomous University of Mexico Tectonic Map of Mexico GIS Project. American Association of Petroleum Geologists GIS Open Files series. <http://www.datapages.com/AssociatedWebsites/GISOpenFiles.aspx>.
- Peacock, S. M. (2003). Thermal structure and metamorphic evolution of subducting slabs. *AGU Geophysical Monograph Series*, 138, 7–22.
- Peña-Domínguez, J. C., Negrete-Aranda, R., Neumann, F., Contreras, J., Spelz, R. M., Vega-Ramírez, L. A., & González-Fernández, A. (2022). Heat flow and 2D multichannel seismic reflection survey of the Devil's Hole geothermal reservoir in the Wagner basin, northern Gulf of California. *Geothermics*, 103, 102415.
- Pilz, J., & Spöck, G. (2008). Why do we need and how should we implement Bayesian kriging methods. *Stochastic Environmental Research and Risk Assessment*, 22, 621–632.
- Polyak, B. G., & Smirnov, Y. B. (1968). Relationship between terrestrial heat flow and the tectonics of the continents. *Geotectonics*, 4, 205–213.
- ProLedesma, R. M. (1991). Chemical geothermometers applied to the study of thermalized aquifers in Guaymas, Sonora, Mexico: A case history. *Journal of Volcanology and Geothermal Research*, 46, 49–59.
- ProLedesma, R. M. (2000). Evaluation of the reconnaissance results in geothermal exploration using GIS. *Geothermics*, 29(1), 83–103.
- ProLedesma, R. M., Sugrobov, V. M., Flores, E. L., Juárez, M., & G., Smirnov, Y. B., Gorshkov, A. P., Bondarenko, V. G., Rashidov, V. A. Nedopekin, L. N., & Gavrilov, V. A. (1989). Heat flow variations along the Middle America Trench. *Marine Geophysical Researches*, 11, 69–76.
- ProLedesma, R. M., Canet, C., Torres-Vera, M. A., Forrest, M. J., & Armienta, M. A. (2004). Vent fluid chemistry in Bahía Concepción coastal submarine hydrothermal system, Baja California Sur, Mexico. *Journal of Volcanology and Geothermal Research*, 137, 311–328.
- ProLedesma, R. M., Torres-Vera, M. A., Rodolfo-Metalpa, R., Ángeles, C., Lechuga Deveze, C. H., Villanueva-Estrada, R. E., Shumilin, E., & Robinson, C. (2013). High heat flow and ocean acidification at a nascent rift in the northern Gulf of California. *Nature Communications*, 4(1388), 1–7.
- ProLedesma, R. M., Espinoza-Ojeda, O. M., Iglesias, E. R., & Arango-Galván, C. (2016). Integration of heat flow measurements and estimations in the construction of Mexico's heat flow map. In *Proceedings of the European geothermal congress 2016, Strasbourg, France, 19–24 September* (pp. 1–4).
- ProLedesma, R. M., Carrillo-de la Cruz, J.-L., Torres-Vera, M. A., Membrillo-Abad, A.-S., & Espinoza-Ojeda, O. M. (2018). Heat flow map and geothermal resources in Mexico. *Terra Digitalis*, 2(2), 1–15.
- ProLedesma, R. M., & Morán-Zenteno, D. (2019). Heat flow and geothermal provinces in Mexico. *Geothermics*, 78, 183–200.
- ProLedesma, R. M., Carrillo de la Cruz, J. L., Torres-Vera, M.-A., & Estradas-Romero, A. (2021). High heat flow at the SW

- passive margin of the Gulf of California. *Terra Nova*, 34(3), 155–162.
- Quintero, M., García, J., & Ocampo, J. D. (2005). Geothermics as an option of alternative source of energy in Baja California, México. In *Proceedings of the world geothermal congress, Antalya, Turkey, April 24–29* (p. 5).
- Reiter, M., Shearer, C., & Edwards, C. L. (1978). Geothermal anomalies along the Rio Grande rift in New Mexico. *Geology*, 6(2), 85–88.
- Reiter, M., & Tovar, J. C. (1982). Estimates of terrestrial heat flow in northern Chihuahua, Mexico, based upon petroleum bottom-hole temperatures. *Geological Society of America Bulletin*, 93(7), 613–624.
- Reyes-Lopez, J. A., Ramirez-Hernandez, J., Vega-Aguilar, M. E., Elders, W., & Campbell-Ramirez, H. (1993). A detailed gravity survey to evaluate the geothermal resource potential near Mexicali airport, Baja California, Mexico. *Geothermal Resources Council Transactions*, 17, 161–166.
- Reyes-Orozco, V. M., Avalos-Tapia, D., García-Tirado, J., Rodríguez-Pineda, E., & Ocampo-Aguilar, F. (2019). Preliminary conceptual model of the Domo San Pedro geothermal field - Western sector of Trans-Mexican Volcanic Belt, Nayarit, Mexico. In *Proceedings of the 44th Workshop on Geothermal Reservoir Engineering, Stanford University, Stanford, California, February 11–13* (pp. 1–8).
- Richards, M., Blackwell, D., Williams, M., Frone, Z., Dingwall, R., Batir, J., & Chickering, C. (2012). Proposed reliability code for heat flow sites. *Geothermal Resources Council Transactions*, 36, 211–217.
- Rosales Rodríguez, J. (2007). *Evaluación Integral de los flujos de calor en el golfo de México* (Master thesis, Instituto Politécnico Nacional), p. 104.
- Sanchez-Zamora, O., Doguin, P., Couch, R. W., & Ness, G. E. (1991). Magnetic anomalies of the Northern Gulf of California: Structural and thermal interpretations. In J. P. Dauphin & B. R. T. Simoneit (Eds.), *The Gulf and Peninsular Province of the Californias* (pp. 377–401). American Association of Petroleum Geologists.
- Šafanda, J., Heidinger, P., Wilhelm, H., & Čermák, V. (2005). Fluid convection observed from temperature logs in the karst formation of the Yucatán Peninsula. *Mexico. Journal of Geophysics and Engineering*, 2(4), 326–331.
- Sclater, J. G., Parsons, B., & Jaupart, C. (1981). Oceans and continents: Similarities and differences in the mechanisms of heat loss. *Journal of Geophysical Research*, 86(B12), 11535–11552.
- Stein, C. A., & Stein, S. (1992). A model for the global variation in oceanic depth and heat flow with lithospheric age. *Nature*, 359, 123–129.
- Sena-Lozoya, E. B., González-Escobar, M., Gómez-Arias, E., González-Fernández, A., & Gómez-Ávila, M. (2020). Seismic exploration survey northeast of the Tres Virgenes Geothermal Field, Baja California Sur, Mexico: A new Geothermal prospect. *Geothermics*, 84, 101743.
- Setianto, A., & Triandini, T. (2013). Comparison of Kriging and inverse distance weighted (IDW) interpolation methods in lineament extraction and analysis. *Journal of Southeast Asian Applied Geology*, 5(1), 21–29.
- Shann, M. (2020). The sureste basin of Mexico: Its framework, future oil exploration opportunities and key challenges ahead. *Geological Society London Special Publications*, 504(1), 119–146.
- Shervais, J. W., Glen, J. M. G., Nielson, D. L., Garg, S., Liberty, L. M., Siler, D., Dobson, P., Gasperikova, E., Sonnenthal, E., Neupane, G., DeAngelo, J., Newell, D. L., Evans, J. P., & Snyder, N. (2017). Geothermal play fairway analysis of the Snake River Plain: Phase 2. *Geothermal Resources Council Transactions*, 41, 2328–2345.
- Shervais, J. W., Glen, J. M. G., Siler, D., Liberty, L. M., Nielson, D., Garg, S., Dobson, P., Gasperikova, E., Sonnenthal, E., Newell, D., Evans, J., DeAngelo, J., Peacock, J., Earney, T., Schermerhorn, W., & Neupane, G. (2020). Snyder Play Fairway Analysis in Geothermal Exploration: The Snake River Plain Volcanic Province. In *Proceedings of the 45th workshop on geothermal reservoir engineering, Stanford University, Stanford, California, February 10–12*, p. SGP-TR-216.
- Smith, D. L. (1974). Heat flow, radioactive heat generation, and theoretical tectonics for northwestern Mexico. *Earth and Planetary Science Letters*, 23, 43–52.
- Smith, D. L., & Jones, R. L. (1979). Thermal anomaly in northern Mexico: An extension of the Rio Grande rift? In R. E. Riecker (Ed.), *Rio Grande rift, tectonics and magmatism* (pp. 269–278). American Geological Union. <https://doi.org/10.1029/sp014p0269>.
- Smith, D. L., Nuckels, C. E., III, Jones, R. L., & Cook, G. A. (1979). Distribution of heat flow and radioactive heat generation in northern Mexico. *Journal of Geophysical Research*, 84(B5), 2371–2379.
- Sourisseau, D., Macías, J. L., García Tenorio, F., Avellán, D. R., Saucedo Girón, R., Bernal, J. P., Arce Saldaña, J. L., & Tinoco Murillo, Z. (2020). New insights into the stratigraphy and ²³⁰Th/U geochronology of the post-caldera explosive volcanism of La Primavera caldera, Mexico. *Journal of South American Earth Sciences*, 103, 102747.
- Suarez-Vidal, F., Armijo, R., Morgan, G., Bodin, P., & Gastil, R. G. (1991). Framework of recent and active faulting in northern Baja California. In J. P. Dauphin & B. R. Simoneit (Eds.), *The Gulf and Peninsular Province of the Californias* (pp. 285–300). American Association of Petroleum Geologists.
- Think GeoEnergy. (2023). Top 10 Geothermal Countries 2022: Installed capacity in Mwe January 2023. <https://www.thinkgeoenergy.com/thinkgeoenergys-top-10-geothermal-countries-2022-power-generation-capacity-mw/>.
- Valdez Moreno, G., Aranda-Gómez, J. J., & Ortega-Rivera, A. (2011). Geoquímica y petrología del campo volcánico de Ocampo, Coahuila, México. *Boletín de la Sociedad Geológica Mexicana*, 63(2), 235–252.
- van Keken, P. E., & King, S. D. (2005). Thermal structure and dynamics of subduction zones: Insights from observations and modeling. *Physics of the Earth and Planetary Interiors*, 149, 1–6.
- Vidal, V. M. V., Vidal, F. V., & Isaacs, J. D. (1978). Coastal submarine hydrothermal activity off northern Baja California. *Journal of Geophysical Research*, 83(B4), 1757–1774.
- Vidal, V. M. V., Vidal, F. V., & Isaacs, J. D. (1981). Coastal submarine hydrothermal activity off northern Baja California 2. Evolutionary history and isotope geochemistry. *Journal of Geophysical Research*, 86(B10), 9451–9468.
- Villanueva-Estrada, R. E., Prol-Ledesma, R. M., Rodríguez-Díaz, A. A., Canet, C., Torres-Alvarado, I. S., & González-Partida, E. (2012). Geochemical processes in an active shallow submarine hydrothermal system, Bahía Concepción, México: Mixing or boiling? *International Geology Review*, 54(8), 907–919.
- Vitarello, I., & Pollack, H. N. (1980). On the variation of continental heat flow with age and the thermal evolution of continents. *Journal of Geophysical Research*, 85(B2), 983–995.
- Von Herzen, R. P. (1963). Geothermal heat flow in the Gulfs of California and Aden. *Science*, 140(3572), 1207–1208.
- Von Herzen, R. P. (1964). Ocean-floor heat-flow measurements west of the United States and Baja California. *Marine Geology*, 1(3), 225–239.
- Wilhelm, H., Heidinger, P., Šafanda, J., Čermák, V., Burkhardt, H., & Popov, Y. (2004). High resolution temperature mea-

- surements in the borehole Yaxcopoil-1, Mexico. *Meteoritics & Planetary Science*, 39(6), 813–819.
- Williams, D. L., Becker, K., Lawver, L. A., & Von Herzen, R. P. (1979). Heat flow at the spreading centers of the Guaymas Basin, Gulf of California. *Journal of Geophysical Research*, 84(B12), 6757–6769.
- Wisian, K. W., & Blackwell, D. D. (2004). Numerical modeling of Basin and Range geothermal systems. *Geothermics*, 33(6), 713–741.
- Ziagos, J. P., Blackwell, D. D., & Mooser, F. (1985). Heat flow in southern Mexico and the thermal effects of subduction. *Journal of Geophysical Research*, 90(B7), 5410–5420.

Springer Nature or its licensor (e.g. a society or other partner) holds exclusive rights to this article under a publishing agreement with the author(s) or other rightsholder(s); author self-archiving of the accepted manuscript version of this article is solely governed by the terms of such publishing agreement and applicable law.